Coordination Chemistry Reviews, 120 (1992) 87–136
Elsevier Science Publishers B.V., Amsterdam

Some synthetic and theoretical aspects of the chemistry of polynuclear transition-metal complexes

Alessandro Bencini and Stefano Midollini
Dipartimento di Chimica, Università degli Studi di Firenze and Istituto per lo Studio della Stereochimica ed Energetica dei Composti di Coordinazione, C.N.R., Florence (Italy)

(Received 15 November 1991)

CONTENTS

ABBREVIATIONS

Et_2Dtc	diethyldithiocarbamate
hfa	hexafluoroacetylacetonate
LS_3^{3-}	trianion of 1,3,5-tris(4,6-dimethyl-3-mercaptophenylthio)-2,4,6-tris (*p*-tolylthio)benzene
napy	1,8-naphthyridine
np_3	tris(2-diphenylphosphinoethyl)amine
salen	*N*,*N*′-bis(salicylaldiminato)ethylenediamine
S_2-dur	durene-α,α'-dithiolate
S_2-o-xyl	*o*-xylene-α,α'-dithiolate
triphos	1,1,1-tris(diphenylphosphinomethyl)ethane

A. INTRODUCTION

Polynuclear molecules containing transition metal and main group bare atoms cemented together, and surrounded by ancillary ligands, constitute a fascinating topic of modern coordination chemistry [1]. When a direct metal–metal bond is present in these molecules they are generally referred to as "clusters". We will use the term cluster in a loose sense to include all molecules formed by a number of metal atoms larger than one. In some compounds, the relative disposition of the metals and ligand atoms resembles the geometry of clusters found in naturally occurring enzymes and they are considered the synthetic analogues of their active sites [2–4]; in other compounds, similarity is found between structural units which are present in the lattice of inorganic solids showing peculiar physical properties (electrical conduction, ferromagnetism, etc.) [5] or which enter into heterogeneous catalytic processes [6]. The chemistry of these molecules and the experimental and theoretical characterization of their physical properties is therefore intrinsically important, the novelty of the synthetic, structural and theoretical aspects issuing a challenge to inorganic chemists.

In order to limit the size of the present article, we must choose a subset of the universe of clusters synthesized up to the present time. Our leading criterion will be to show the contribution of the Florence research groups in this area. A huge part of the research interest of Prof. Luigi Sacconi, to whom this special edition of *Coordination Chemistry Reviews* is dedicated, in the years 1960–1980 was devoted to the synthesis and the structural and physico-chemical characterization of 3d-metal complexes. Among the systems investigated, metal–chalcogen complexes received particular attention; therefore in Sect. B we will deal with polynuclear iron, cobalt and nickel–chalcogen species containing terminal ligands such as halides, thiolates, phosphines, etc. Organometallic species containing metal–carbon, hydrogen or nitrosyl bonds will not be considered. In this section, emphasis will be placed on the synthetic routes which lead to the formation of clusters.

Modern synthetic strategies in coordination chemistry, generally involve the use of sophisticated reagents and sterically hindered ligands or ligands with varied donor atoms in order to stabilize particular coordination geometries and/or to promote special chemical processes. On the other hand, the synthesis of metal–chalcogen clusters is basically achieved by the spontaneous self-assembly of simple inorganic reagents. Later, new compounds can be obtained by exploiting the reactivity of the parent clusters. Although, just for these reasons the pursuit of the metal–chalcogen chemistry remains a largely empirical approach, we will try to discuss some synthetic strategies. The structural features of this class of compound have already been carefully treated in the literature, and we will therefore give only a brief description of them, but we will report the results of the most significant investigations of their magnetic properties.

The aggregation of paramagnetic ions in the presence of ligands can likely lead to the formation of polynuclear paramagnetic species and Sect. C will give a brief account of the electronic structure of paramagnetic clusters. The magnetic properties of polynuclear transition metal compounds have attracted the interest of several researchers for a long time. This is a consequence of the fact that some of these compounds have a number of electronic states, differing in their total spin, populated at the same temperature and possess a peculiar temperature dependence of the magnetization which give rise to ferro-, antiferro, ferri-, etc. magnetism at the molecular level. This behaviour is opposite to that found in many other molecular compounds where only one spin state is thermally populated at room temperature, either a singlet, diamagnetic, or a paramagnetic state. These properties have been ascribed to so-called "super-exchange interactions". The nature of the chemical bond between the transition metal ion and the intervening ligands is, of course, responsible for these interactions and in Sect. C we will be concerned with the phenomenological description of these effects and with their interpretation at the electronic level.

These properties are rather peculiar to the complexes of the first row transition metals and Prof. Sacconi always looked to this research as a natural complement to chemical synthesis and strongly encouraged theoretical development in this field. This is the main reason why we collected together chemical synthesis and quantum mechanical aspects, which, at a first glance, may seem to be the subjects of two different reviews. The reader will note that most of the compounds described in Sect. B have not yet been fully theoretically characterized due to the complexity of their geometries and to the large number of electrons which makes any quantum mechanical description of their electronic structure difficult. The full experimental and theoretical characterization of large transition-metal molecular clusters is a challenge for future research.

In Sect. C, we will not give any account of the physico-chemical techniques used to determine experimentally the magnetic structure of the clusters examined, which are treated in the review article by Benelli and Gatteschi in this same issue. Also, we will limit ourselves to the description of the interactions at the molecular level and we will not consider solid state effects for which a quantitative theoretical description is still far from being available. Knowledge of the mechanisms which govern the electronic interactions at the molecular level constitutes the basis for the comprehension of solid state effects and for the description of the magnetic properties of those clusters found in living organisms.

B. CHEMISTRY OF IRON, COBALT AND NICKEL–CHALCOGEN CLUSTERS

The iron–sulphur proteins and analogous clusters have been extensively reviewed [2–4,7,8]. Fenske recently reported the results obtained by his group on cobalt- and nickel–chalcogen systems [9].

TABLE 1

Bi, tri- and tetrametallic clusters

Core[a]	Compound	Synthesis[b]	Formal Oxidation State	Magnetic Properties[c]	Ref.
bimetallic					
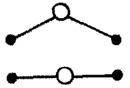 1 $M_2(\mu_2\text{-}E)$					
	$[Fe_2S(salen)_2]$	a1,a5	Fe(III)	J=352	10
	$[Co_2S(np_3)_2]$		Co(I)	D	11
	$[Ni_2S(triphos)_2](BPh_4)_2$	a4	Ni(II)	D	11
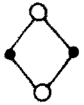 2 $M_2(\mu_2\text{-}E)_2$					
	$[Fe_2S_2(S_2\text{-}o\text{-}xyl)_2](Et_4N)_2$	a3	Fe(III)	J=300	12
	$[Fe_2S_2Cl_4](Et_4N)_2$	d	Fe(III)	J=340	13
	$[Fe_2S_2(o,o'\text{-}C_{12}H_8O_2)_2](Et_4N)_2$	d	Fe(III)	AF	14
	$[Co_2S_2(triphos)_2]$	b	Co(II)	D	15
	$[Co_2S_2(triphos)_2](BPh_4)$	a4	1Co(II)1Co(III)	S=1/2	15
	$[Co_2S_2(triphos)_2](BPh_4)_2$	b	Co(III)	D	15

trimetallic					
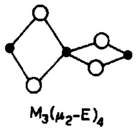 **3**					
	$[Fe_3S_4(SEt)_4](Et_4N)_3$	a1	Fe(III)	$J_{12}=J_{23}=300$, $-100\leq J_{13}\leq 100$	16,17
	$[Fe_3Se_4(SEt)_4](Et_4N)_3$	a1,d	Fe(III)	$S=5/2$	18
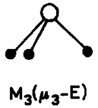 **4**					
	$[Fe_3S(S_2\text{-dur})_3](Et_4N)_2$	a2	Fe(II)		19
	$[Fe_3S(S_2\text{-}o\text{-xyl})_3](Et_4N)_2$	a2	Fe(II)	$\mu_{eff}(301\ K)=3.95$	20
	$[Co_3S(S_2\text{-}o\text{-xyl})_3](Et_4N)_2$		Co(II)	$\mu_{eff}(295\ K)=3.46$	20
	$[Ni_3S(SMe)_6](Me_4N)_2$		Ni(II)	D	21
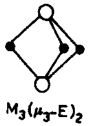 **5**					
	$[Fe_3S_2(WS_4)_3](Ph_4P)(Et_4N)_3$		Fe(II)	AF	22

TABLE 1 (continued)

Core[a]	Compound	Synthesis[b]	Formal Oxidation State	Magnetic Properties[c]	Ref.
	$[Ni_3S_2(PEt_3)_6](BPh_4)_2$	a4	Ni(II)	D	23
	$[Ni_3Se_2(PEt_3)_6](BPh_4)_2$	a4	Ni(II)	D	24
	$[Ni_3Te_2(PEt_3)_6](BPh_4)_2$	a4	Ni(II)	D	25
	$[Ni_3S_2(PEt_3)_5(SH)](BPh_4)$	a4	Ni(II)	D	26
	$[Ni_3S_2(PEt_3)_5Cl](BPh_4)$	a5,d	Ni(II)	D	25
	$[Ni_3S_2(PEt_3)_2(Et_2Dtc)_2]$	d	Ni(II)	D	27
tetrametallic					
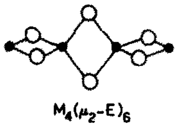 **6**	$[Fe_4S_6(SEt)_4](Et_4N)_4$	a1	Fe(III)	AF	28
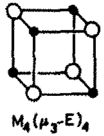 **7**					
	$[Fe_4S_4(SPh)_4](Et_4N)_3$	b	3Fe(II)1Fe(III)	J=110, α=J'/J=1.5-1.7;	29,30
	$[Fe_4Se_4(SPh)_4](Et_4N)_3$	b	3Fe(II)1Fe(III)	S=1/2 J=65, α=1.7;	31
	$[Fe_4Te_4(SPh)_4](Et_4N)_3$	a2	3Fe(II)1Fe(III)	S=3/2 J=31, α=1.8;	30
	$[Fe_4S_4(SPh)_4](Et_4N)_2$	a1	2Fe(II)2Fe(III)	J_1=544, J_2=450,	32
	$[Fe_4Se_4(SPh)_4](Me_4N)_2$	a3	2Fe(II)2Fe(III)	J_3=500 AF	33
	$[Fe_4S_4(OPh)_4](Et_4N)_2$	d	2Fe(II)2Fe(III)	J=340	34,35

$[Fe_4S_4Cl_4](Et_4N)_2$	d	2Fe(II)2Fe(III)	J=316	36
$[Fe_4S_4(SH)_4](Ph_4P)_2$	a4	2Fe(II)2Fe(III)	μ_{eff}(295K)=4.4.	37
$[Fe_4S_4Cl_3(Et_2Dtc)](Ph_4P)_2$	d	2Fe(II)2Fe(III)	AF	38
$[Fe_4S_4(LS_3)Cl](Ph_4P)_2$	d	2Fe(II)2Fe(III)	AF	39
$[Fe_4S_4(S\text{-}2,4,6\text{-}(i\text{-}Pr)_3C_6H_2)_4](Bu_4N)$	b	1Fe(II)3Fe(III)	S=1/2	40
$[Fe_3NiS_4(PPh_3)(SEt_4)_3](Et_4N)_2$	c	2Fe(II)1Fe(III)1Ni(II)	S=3/2	41
$[Co_4Se_4(PPh_3)_4]$	a5	Co(II)	D	42
$[Ni_4Se_4(PPh_3)_4]$	a5	Ni(II)	D	9

---

[a] Metal = ●; chalcogen = ○.

[b] The paragraphs of sections B.ii are indicated; unique syntheses are not reported.

[c] The overall magnetic behaviour of the solid compounds is indicated. The nature of the ground state is reported as S = spin state when it is explicitly mentioned. We report the measured values of exchange coupling constants with the Hamiltonian $H = \Sigma_{i \neq j} J_{ij} S_i . S_j$ when available; all the values are expressed in cm^{-1}. The μ_{eff} is expressed in μ_B. AF and D respectively means overall antiferromagnetic coupling and diamagnetism.

(i) Structural and magnetic aspects

At least 19 structural types of cluster with metallic nuclearity ranging from two to nine have been identified so far. They are collected in Tables 1 and 2. Some other compounds of higher nuclearity, whose cores are likely formed by the condensation of two or more of the above structural types, and some examples of giant frameworks of unique structural type will also be considered. An account of the physical properties of those clusters which have been characterized will also be given.

The structures of the most relevant bi, tri, and tetrametallic cluster cores (**1**–**7**) are shown in Table 1.

Dinuclear species with one or two chalcogen bridges are known. Iron(III) Schiff base complexes show different bent sulphur bridges (Fe–S–Fe angle in the range 121°–174°) depending on the steric requirements of the ligands [68]. In the complex $[Fe_2S(SALen)_2]$, (Fig. 1) the Fe–S–Fe bridge (122°) is slightly asymmetric with Fe–S bond distances of 215.0(2) pm and 219.0(2) pm, respectively [10]. The dependence of the magnetic properties of $[Fe_2X]^{4+}$ units on the bridging angles has been investigated by Mukherjee et al. [68]. A linear arrangement of the two metals and of the bridging chalcogen, M_2E (**1**) is found in the tripodal phosphine nickel(II) and cobalt(I) complexes shown in Fig. 2 [11]. The metal–sulphur bond length (203.4(2) pm) is rather short and indicates a strong metal–ligand interaction. The complexes are diamagnetic.

The double bridging arrangement, M_2E_2 (**2**) is exemplified in Fig. 3 by the structure of the complex $[Co_2S_2(triphos)]$ [15]. Several iron(III) compounds have been synthesized with the intent of finding synthetic models of the two-iron two-sulphur clusters present in some iron–sulphur proteins. The electronic structure of these bimetallic clusters has been investigated through electronic, Mössbauer, cyclic voltammetry, ^1H NMR and EPR spectroscopy [2,3]. In all cases, an antiferromagnetic coupling between the iron centres is operative with an exchange coupling constant, J, in the range 300–400 cm^{-1} (see Sect. C for the definition of J).

The structure of the type **3** trinuclear cluster $[Fe_3S_4(SPh)_4]^{3-}$, shown in Fig. 4, is closely related to type **2** structures, having a linear array of three pseudo-tetrahedral iron atoms doubly bridged by sulphur [16]. The magnetic structure of clusters with a linear arrangement of the iron atoms has been investigated carefully by Girerd et al. [17]. In the compounds investigated, the ground state was found to be a spin sextet ($S = 5/2$) arising from antiferromagnetic exchange interactions between adjacent high spin ($S_1 = S_2 = S_3 = 5/2$) iron(III) ions ($J_{12} = J_{23} \approx 300\ cm^{-1}$) and smaller interactions between terminal atoms ($-100 \leqslant J_{13} \geqslant 100\ cm^{-1}$). Other trimetallic clusters show a triangular arrangement of the three metals, capped (**4**) or bicapped (**5**), by one or two chalcogens, respectively. In Fig. 5, the structure of the complex $[Fe_3S(S_2\text{-dur})_3]^{2-}$ is shown [19]. In these complexes [20,21], a discrete pyramidal $M_3(\mu_3\text{-S})$ fragment is found, which is rather uncommon for inorganic complexes and is more easily encountered in organometallic compounds. The complex

TABLE 2

Hexa-, hepta-, octa- and nonametallic clusters

Core[a]	Compound	Synthesis[b]	Formal Oxidation State	Magnetic Properties[c]	Ref.
hexametallic					
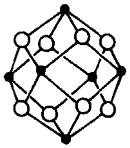 **8** $M_6(\mu_3\text{-}E)_8$					
	$[Fe_6S_8(PEt_3)_6](PF_6)$	a4	1Fe(II)5Fe(III)	S=7/2	43,44
	$[Fe_6S_8(PEt_3)_6](BPh_4)_2$	a4	Fe(III)	AF	45
	$[Co_6S_8(PEt_3)_6]$	b	2Co(II)4Co(III)	D	46
	$[Co_6Se_8(PPh_3)_6]$	a5	2Co(II)4Co(III)	D	42
	$[Co_6Te_8(PEt_3)_6]$	a6	2Co(II)4Co(III)	D	47
	$[Co_6S_8(PEt_3)_6](BPh_4)$	a4	1Co(II)5Co(III)	S=1/2	44,48
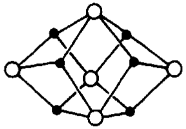 **9** $M_6(\mu_4\text{-}E)_3(\mu_3\text{-}E)_2$					
	$[Ni_6Se_5(PPh_3)_6]$	a5	2Ni(I)4Ni(II)	D	49

TABLE 2 (continued)

Core[a]	Compound	Synthesis[b]	Formal Oxidation State	Magnetic Properties[c]	Ref.
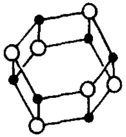 **10** $M_6(\mu_3\text{-}E)_6$					
	$[Fe_6S_6(SC_6H_4\text{-}p\text{-}Me)_6](Et_4N)_3$	d	3Fe(II)3Fe(III)	S=1/2	50
	$[Fe_6S_6(OC_6H_4\text{-}p\text{-}Me)]_6(Et_4N)_3$	d	3Fe(III)3Fe(III)	S=1/2	50a
	$[Fe_6S_6Cl_6](Et_4N)_3$	a1	3Fe(II)3Fe(III)	S=1/2	50a
	$[Fe_6S_6Cl_6](Ph_4P)_2$	b	2Fe(II)4Fe(III)	AF	51
	$[Fe_6S_6I_6](Et_4N)_2$	a1	2Fe(II)4Fe(III)		52
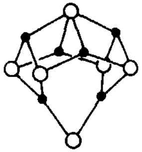 **11** $M_6(\mu_4\text{-}E)(\mu_3\text{-}E)_4(\mu_2\text{-}E)$					
	$[Fe_6S_6(PEt_3)_6](BF_4)$	a5	5Fe(II)1Fe(III)	S=1/2	53
	$[Fe_6S_6(PEt_3)_4(SPh)_2]$	a5,c	4Fe(II)2Fe(III)	S=1	54
	$[Fe_6S_6(PEt_3)_4Cl_2]$	a5,c	4Fe(II)2Fe(III)	S=1	55
	$[Fe_6Se_6(PEt_3)_4Cl_2]$	a5,c	4Fe(II)2Fe(III)	S=1	55

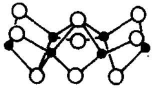 **12** $M_6(\mu_4\text{-}E)(\mu_3\text{-}E)_2(\mu_2\text{-}E)_6$					
	$[Fe_6S_9(S\text{-}t\text{-}Bu)_2](Me_3BzN)_4$	a2	3Fe(II)3Fe(III)	AF	56
	$[Fe_6S_9(SBz)_2](Et_4N)_4$	a6	3Fe(II)3Fe(III)	AF	57
	$[Fe_6Se_9(SMe)_2](Et_3BzN)_4$	a6	3Fe(II)3Fe(III)	AF	58
heptametallic					
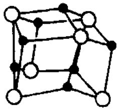 **13** $M_7(\mu_4\text{-}E)_3(\mu_3\text{-}E)_3$					
	$[Fe_7S_6(PEt_3)_4Cl_3]$	a5	6Fe(II)1Fe(III)	$\mu_{eff}(298K)=3.95^d$	59
	$[Co_7S_6(PPh_3)_5Cl_2]$	a5	Co(II)	*e*	60
	$[Co_7S_6(PPh_3)_4Cl_3]$	a5	6Co(II)1Co(III)	D	9
octametallic					
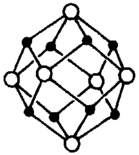 **14** $M_8(\mu_4\text{-}E)_6$					
	$[Fe_8S_6I_8](Et_4N)_3$	c	7Fe(II)1Fe(III)		61

TABLE 2 (continued)

Core[a]	Compound	Synthesis[b]	Formal Oxidation State	Magnetic Properties[c]	Ref.
	$[Co_8S_6(SPh)_8](Et_4N)_5$	b	1Co(I)7Co(II)	S=1/2	62
	$[Co_8S_6(SPh)_8](n\text{-}Pr_4N)_4$	a3	Co(II)	AF	62
	$[Ni_8S_6(PPh_3)_8]$	b	4Ni(I)4Ni(II)	D	63
	$[Ni_8S_6(PPh_3)_6Cl_2$	a5	2Ni(I)6Ni(II)	D	60
	$[Fe_3Ni_5S_6I_8](NH_4)_4$	c	3Fe(II)2Fe(III)3Ni(II)	D	64
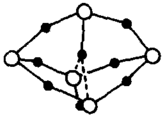 15 $M_8(\mu_3\text{-}E)_5$					
	$[Ni_8S_5(PPh_3)_7]$	a5	6Ni(I)2Ni(II)	D	60
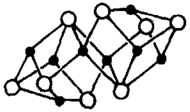 16 $M_8(\mu_4\text{-}E)_2(\mu_3\text{-}E)_6$					
	$[Co_8Se_8(PPh_3)_6]$	a5	Co(II)	D	65
	$[Co_8Se_8(PPh_3)_6][CoCl_3(PPh_3)]$	a5	7Co(II)1Co(III)	e	65

nonametallic					
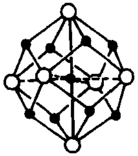 **17** $M_9(\mu_4\text{-}E)_6$	$[Ni_9Te_6(PEt_3)_8]$	a6	6Ni(I)3Ni(II)	D	66
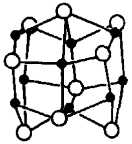 **18** $M_9(\mu_4\text{-}E)_3(\mu_3\text{-}E)_6$	$[Ni_9S_9(PEt_3)_6](BPh_4)_2$	a4	7Ni(II)2Ni(III)	D	67
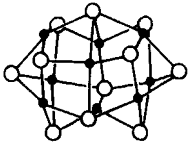 **19** $M_9(\mu_4\text{-}E)_3(\mu_3\text{-}E)_8$	$[Co_9Se_{11}(PPh_3)_6]$	a5	5Co(II)4Co(III)	e	42

---

[a] Metal = ●; chalcogen = ○.

[b] The paragraphs of section B.ii are indicated.

[c] The overall magnetic behaviour of the solid compounds is indicated. The nature of the ground state is reported as S = spin state when it is explicitly mentioned. AF and D respectively mean overall antiferromagnetic coupling and diamagnetism.

[d] $CDCL_3$ solution.

[e] The compound is reported as paramagnetic without any indication of experimental results.

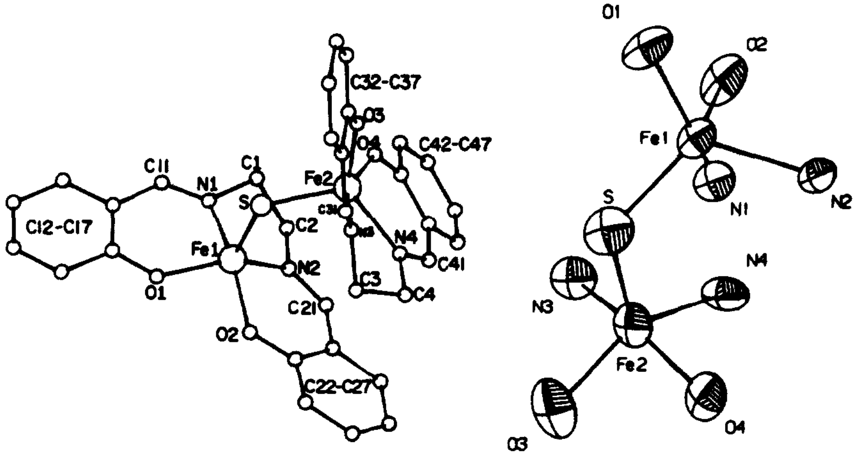

Fig. 1. Structure and ORTEP view of the skeleton of $[Fe_2S(salen)_2]$. (From ref. 10.)

$[Fe_3S_2(WS_4)_3]^{4-}$ is the only example of an iron complex containing the trigonal bipyramidal core 5 [22]. On the other hand, several clusters of nickel(II) have been reported [23–27]. In Fig. 6, the structure of the complex $[Ni_3S_2(PEt_3)_6]^{2+}$ [23] is shown. All these compounds are diamagnetic and can be described as being formed by three square-planar $Ni_2E_2L_2$ moieties sharing two μ_3-E ligands.

The linear arrangement of the metals in tetrametallic clusters (6) is still rare [28], the most common geometry being the cubane-type (7). A long series of compounds with geometries derived from the ideal cubane has indeed been characterized and their structural features and properties have been extensively reviewed [3,9,29–42]. Recently, the crystal structures of iron–selenium cubane clusters have been determined [18] and the main distortions of the $[Fe_4Se_4]^{2+,+}$ cores from cubic arrangement have been discussed.

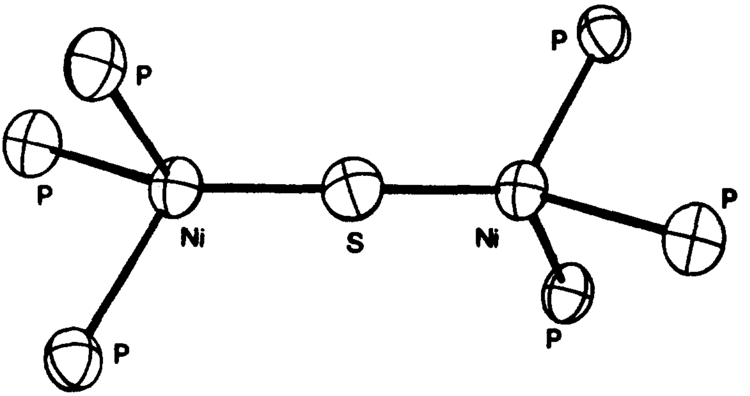

Fig. 2. ORTEP drawing of the skeleton of $[Ni_2S(triphos)_2]^{2+}$. (From ref. 11.)

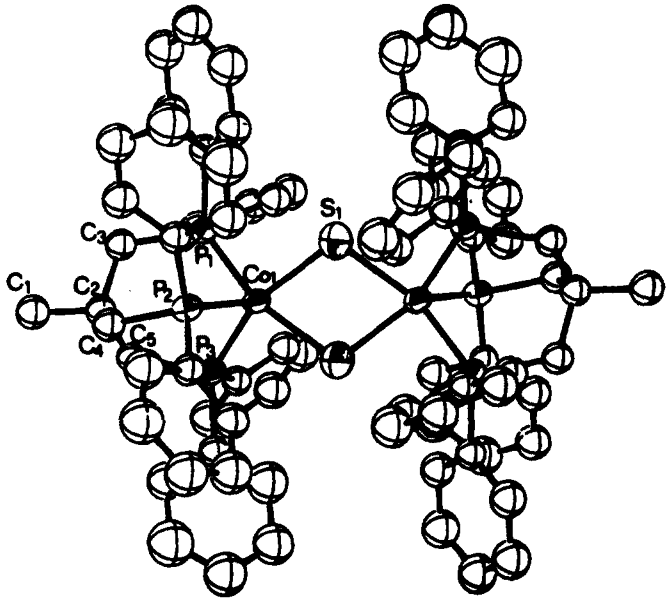

Fig. 3. Perspective view of $[Co_2S_2(triphos)_2]$. (From ref. 15.)

The nature of the ground state of complexes containing the $[Fe_4X_4]^+$ (X = S, Se, Te) core, which is formed by three iron(II) and one iron(III) centres, has been studied by Mössbauer, magnetic and EPR techniques [2,30,31,69–71]. In Table 1, we report the values measured for the exchange coupling constants (when available) relative to the magnetic coupling between two iron(II) centres (J) and between iron(II) and iron(III) (J') according to the hamiltonian used in Sect. C. The exact ground state, either $S = 1/2$, $S = 3/2$ or an admixture of them, was found to be dependent on very subtle factors, not yet rationalized, such as the nature of the counterions. In these and other cubane-like clusters, such as those containing the core $[Fe_4S_4]^{2+,3+}$, valence delocalization ("double exchange") was found to be important in determining

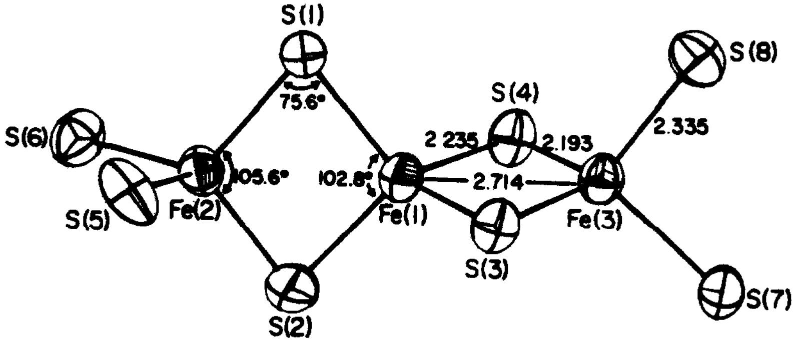

Fig. 4. ORTEP view of the skeleton of $[Fe_3S_4(SPh)_4]^{3-}$. (From ref. 16.)

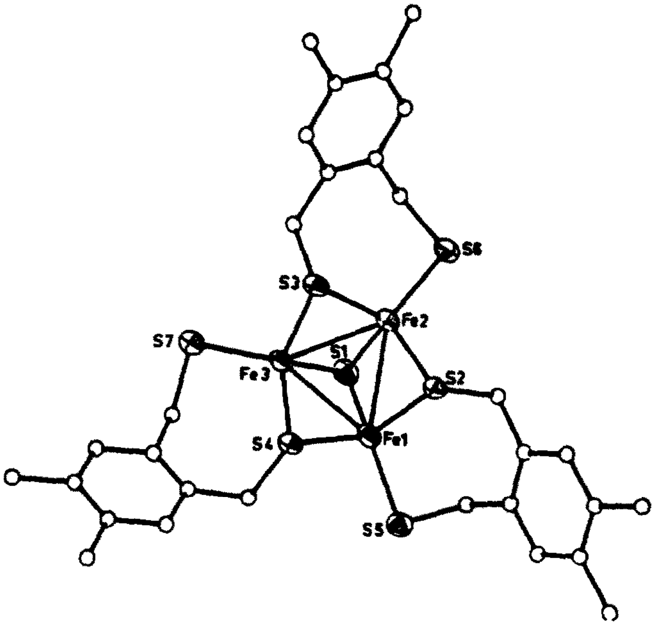

Fig. 5. ORTEP view of $[Fe_3S(S_2\text{-dur})_3]^{2-}$. (From ref. 19)

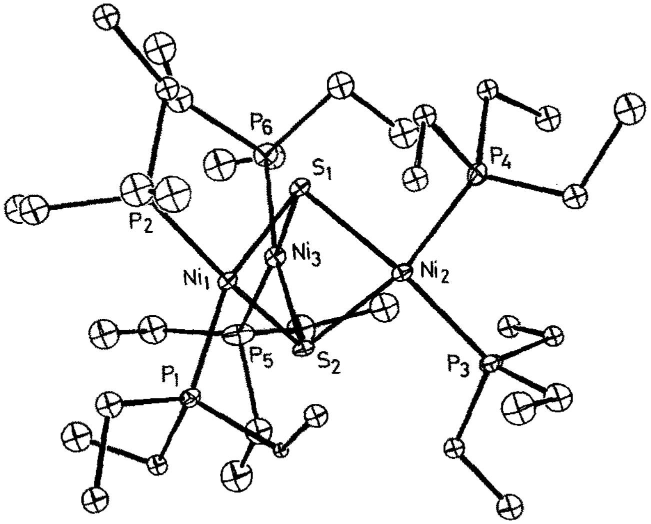

Fig. 6. ORTEP view of $[Ni_3S_2(PEt_3)_6]^{2+}$. (From ref. 23.)

the total spin ground state and the detailed spin coupling pattern. We cannot enter here in a full characterization of the magnetic structure of these clusters, but it was generally observed that the overall interaction is antiferromagnetic. A brief account of the double exchange is given in Sect. C, where we also give principal references to the studies performed on the iron–sulphur cubane systems.

Hexa, hepta, octa, and nona-metallic clusters (**8–19**) are reported in Table 2.

Four types of hexametallic species have been isolated. The most symmetric structure (**8**) can be described as being formed by an octahedron of metals with eight chalcogens triply bridging the octahedral faces. The eight chalcogens lie at the vertex of a cube [42,43,45–48]. An example of this structure is given in Fig. 7 for the cation $[Fe_6S_8(PEt_3)_6]^{2+}$ [45]. The iron atoms lie at the vertex of an almost perfect octahedron (average Fe—Fe distance = 262 pm). The actual site symmetry of the complexes obtained with both iron and cobalt depends on the nature of the counter-ion. For the hexafluorophosphate derivatives, C_3 site symmetries have been found [43,44]. The magnetic properties of compounds of this series are rather peculiar and are briefly mentioned at the end of Sect. C.

A unique example of a trigonal prismatic core M_6S_5 (**9**) has been found in the complex $Ni_6Se_5(PPh_3)_6$. The longest Ni—Ni bond distances are those between the nickel atoms on the triangular faces of the prism [49].

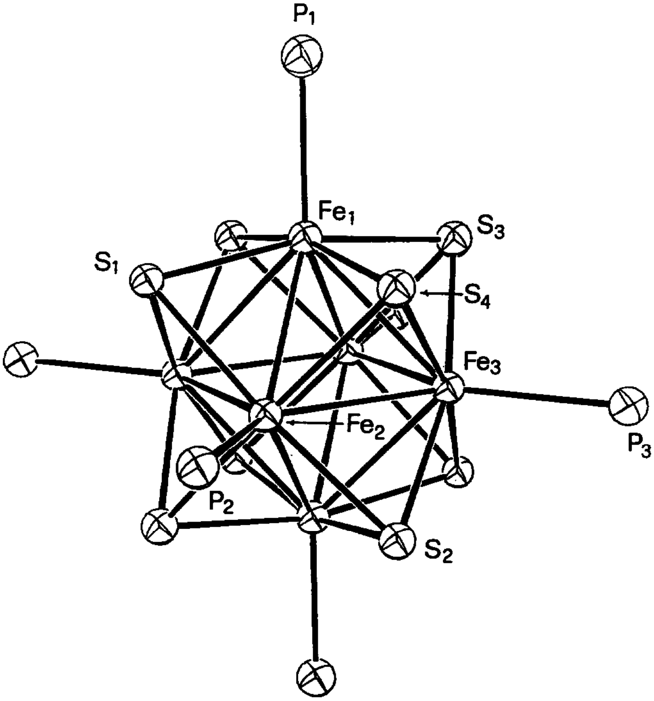

Fig. 7. ORTEP view of $[Fe_6S_8(PEt_3)_6]^{2+}$. (From ref. 45.)

The structure of the prismane core Fe_6S_6 (**10**) can be described as being formed by three rhombic Fe_2S_2 units linked to yield a distorted hexagonal prismatic arrangement [50–52]. In Fig. 8, the molecular structure of $[Fe_6S_6I_6]^{2-}$ is shown [52].

The basket-like Fe_6S_6 core (**11**), as found in the compound $[Fe_6S_6(PEt_3)_6]^+$, can be viewed as being formed by six non-planar Fe_2S_2 moieties fused together to form an open basket with a bridging Fe(μ_2-S)Fe group, with bond angle 75.5°, as the "handle". In this structure, which approaches an idealized C_{2v} symmetry, three inequivalent bridges are present, namely μ_2-S, μ_3-S, and μ_4-S [53–55].

Three types of bridging chalcogen atom are also present in the Fe_6E_9 structural type **12** [56–58]. This is exemplified in Fig. 9 by the complex $[Fe_6Se_9(SMe)_2]^4$ [58]. The core of the cluster is formed by eight Fe_2Se_2 moieties fused to form four Fe(μ_2-Se)(μ_3-Se)Fe, two Fe(μ_2-Se)(μ_4-Se)Fe and two Fe(μ_3-Se)(μ_4-Se)Fe subunits.

The monocapped prismane **13** is the only heptametallic structural type so far reported [9,59,60].

Among the octametallic clusters, the structure in which a cube of eight metals is penetrated by an octahedron of sulphur (**14**) is surely the most symmetric [61–64]. An example is given in Fig. 10, where the molecular structure of the complex $[Fe_8S_6I_8]^{4-}$ is shown [61]. This molecular arrangement is similar to that found in M_6E_8 cluster of type **8** in which the position of the metals and of the chalcogens is exchanged. Interestingly, the structure of **14** is topologically related to those of **10** and **13** [59], as shown in Fig. 11.

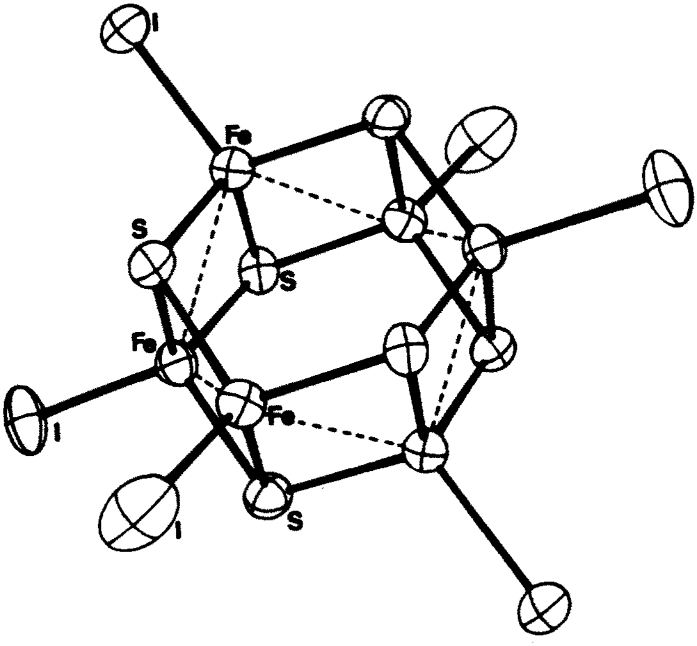

Fig. 8. Structure of $[Fe_6S_6I_6]^{2-}$. (From ref. 52.)

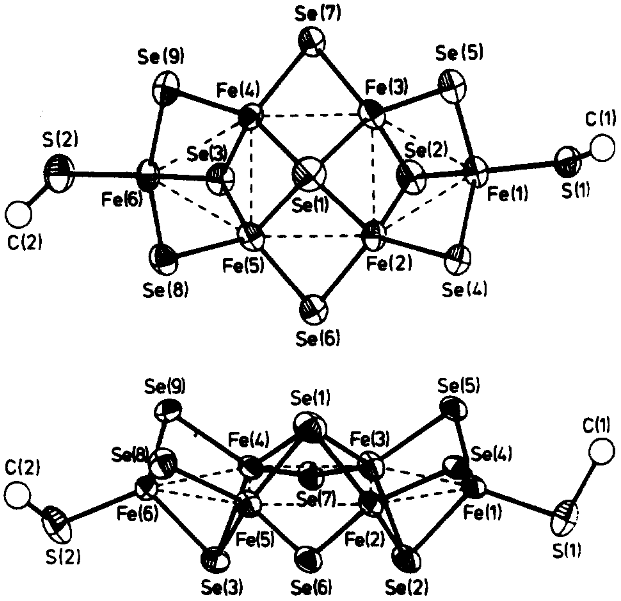

Fig. 9. Two views of $[Fe_6Se_9(SMe)_2]^{4-}$. (From ref. 58.)

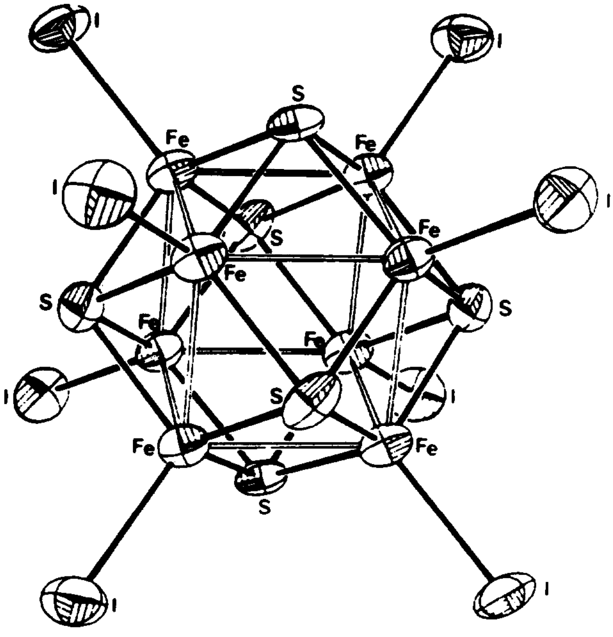

Fig. 10. ORTEP view of $[Fe_8S_6I_8]^{3-}$. (From ref. 61.)

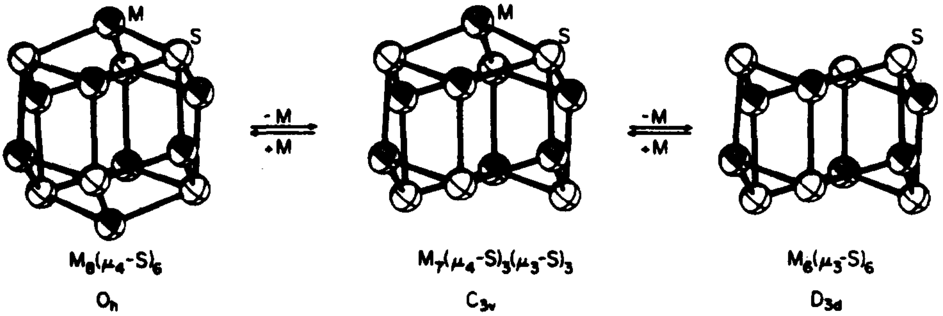

Fig. 11. Structural relationships among M_6S_6, M_7S_6, and M_8S_6 cores. (From ref. 59.)

Two unique structures of octametallic clusters are shown in Figs. 12 and 13. One of these clusters, **15**, is formed by two Ni_5 trigonal-bipyramids with a common edge [60]; the other, **16**, is formed by two trans Co_5 square-pyramids with a common edge [65].

Three examples of nonametallic clusters have been reported so far. The core M_9E_6 (**17**) found in the complex $Ni_9Te_6(PEt_3)_6$, is closely related to the octametallic complex of type **14**, with one metal atom located at the centre of the structural framework [67]. In the cores M_9E_9 (**18**) and M_9E_{11} (**19**) found in the complexes $[Ni_9S_9(PEt_3)_6]^{2+}$ [67], shown in Fig. 14, and $[Co_9Se_{11}(PPh_3)_6]$ [42], respectively, the metal arrangement can be described as being formed by the condensation of two octahedra (**8**) sharing one face. The cores **8**, **17**, **18**, and **19** are closely related to structural units which have been found in the Chevrel phases of molybdenum

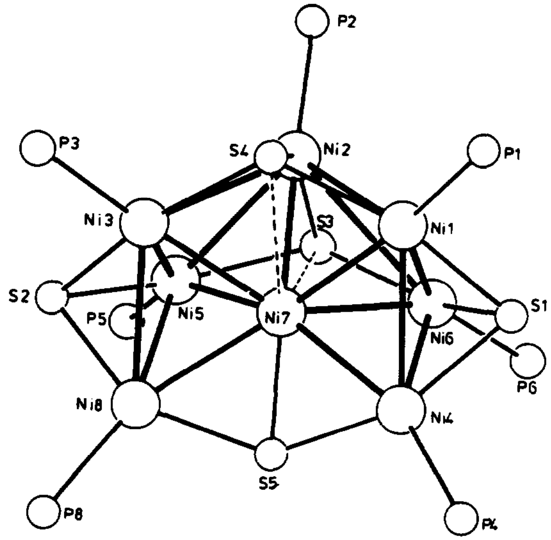

Fig. 12. Molecular structure of $[Ni_8S_5(PPh_3)_7]$. (From ref. 60.)

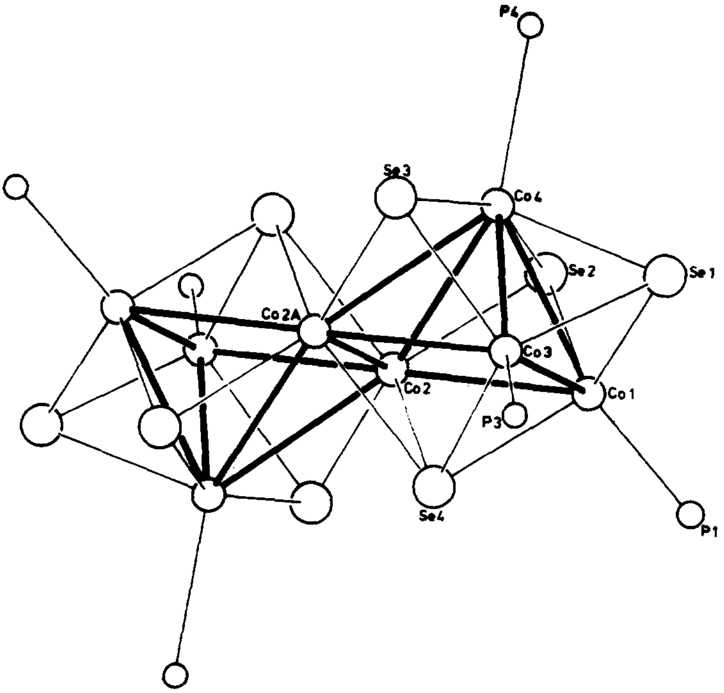

Fig. 13. Molecular structure of $[Co_8S_8(PPh_3)_6]$. (From ref. 65.)

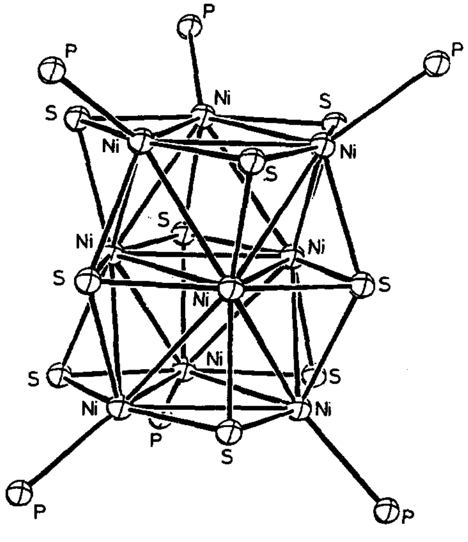

Fig. 14. Inner core of $[Ni_9S_9(PEt_3)_6]^{2+}$. (From ref. 67.)

chalcogenides, most of which were found to be high-field and high-temperature superconductors [5]. Each cluster in these solids can be viewed as a combination of a cube of chalcogens and an octahedron of metals.

Few examples of clusters having metallic nuclearity larger than nine have been reported so far. The complexes [49] $[Ni_{12}Se_{12}(PEt_3)_6]$ and $[Ni_{15}Se_{15}(PPh_3)_6]$ represent an extension of the structural types **18** and **19**, being topologically formed by the condensation of three and four octahedra of metals, respectively, having common faces.

Quite recently, giant clusters of unique exotic structure, $[Na_2Fe_{18}S_{30}]^{8-}$ [72] (Fig. 15), $[Na_9Fe_{20}Se_{38}]^{9-}$ [73], $[Ni_{20}Te_{18}(PEt_3)_{12}]$ [66], $[Ni_{34}Se_{22}(PPh_3)_{10}]$ [42] (Fig. 16) have been reported. This shows how this fascinating field of inorganic chemistry can be developed.

(ii) Synthetic procedures

The basic strategy to most initial metal–chalcogen cluster syntheses consists of the thermodynamically controlled reaction of simple inorganic reagents. Thus a reactant mixture containing a metal source (element metal, salt, complex), a source of the chalcogen E (elemental E, E^{2-}, EH^-, EH_2, $E(SiMe_3)_2$, etc.), an ancillary ligand (SR^-, X^-, PR_3), and a cation or anion to counterbalance the charge of the cluster, is allowed to react to form products, which are the most thermodynamically stable under the condition of the experiment. In some cases, kinetics control the formation of cluster species, which are generally metastable and spontaneously rearrange to form the thermodynamically stable complexes. The term "spontaneous

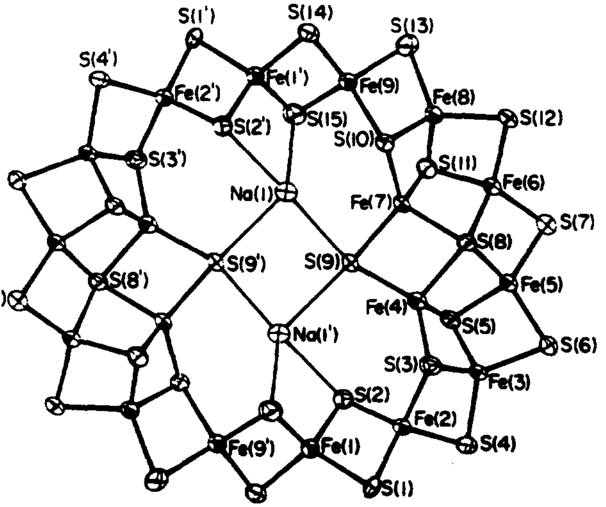

Fig. 15. Structure of $[Na_2Fe_{18}S_{30}]^{8-}$. (From ref. 72.)

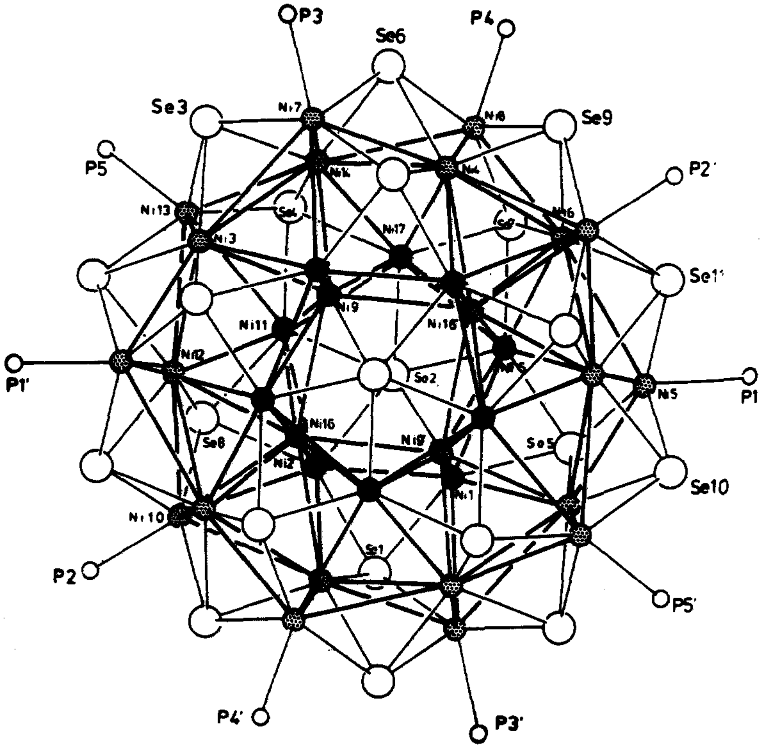

Fig. 16. Molecular structure of $[Ni_{34}Se_{22}(PPh_3)_{10}]$. (From ref. 42.)

self-assembly" has been applied to these processes first by Ibers and Holm [74] as a reminder of the thermodynamic origin of cluster formation.

The actual nature of the products of a given reaction strictly depends on experimental conditions such as the relative amount of reagents, the nature of the solvent, the temperature and the nature of the counterion. Redox processes are also often involved in the reaction mechanism, sometimes leading to species in which a non-integral oxidation number must be attributed to the metals ("mixed valence" compounds).

The parent clusters so assembled can in turn be used to form new compounds by exploiting their reactivity. Thus the oxidation or the reduction of the clusters can afford products with different oxidation states. The coupling of two identical or different clusters is a potential method to construct a new polynuclear species with different nuclearity. Finally, terminal ligand exchange reactions on clusters, when possible, allow the incorporation of virtually any desired ligand or combination of ligands.

(a) Spontaneous self-assembly reactions

Rigorous classification appears impossible since apparently very similar reactions can lead to the isolation of different products, whereas some reactions give unique products. We have therefore separated the self-assembly reactions according to the chalcogen source into sections (1)–(6).

(1) Elemental chalcogens, E, as chalcogen source. The reaction systems $FeCl_3$ (or $FeCl_2$)/ER^-/E (E = S, Se) in non-aqueous solutions have been widely used to synthesize iron–chalcogen clusters ranging in metal nuclearity from 2 to 6. Holm and coworkers [75] systematically explored these reactions and some general statements can now be formulated. Two factors appear to decide the general development of the reaction: (i) the molar ratios between the reagents and (ii) the protic or aprotic nature of the solvent and, in some cases, also the nature of the SR^- anion and the temperature.

The mixtures $FeCl_3/SR^-/S$ have been found to react in protic solvents with the stoichiometry [76]

$$4FeCl_3 + 14SR^- + 4S \rightarrow [Fe_4S_4(SR)_4]^{2-} + 5RSSR + 12Cl^-$$

The process occurs via the reaction sequences reported in Scheme 1 according to the actual molar ratios between the reagents and the nature of the solvent. In aprotic solvents when $FeCl_3 \geqslant 5SR^-$, the reaction stops at the dinuclear species, while in protic solvents, the cubane-like cluster is always obtained [75]. In the case of $FeCl_2$ ($FeCl_4^{2-}$)/SR^-/S, similar reactions occur as shown in Scheme 2, reactions (1) [77] and (2) [78]. Reaction (3) shows an example of the influence of the nature of the counterion [79]. The oxidation of RS^- to RSSR and the oxidative addition of E to Fe(II) thiolate complexes such as $[Fe(SR)_4]^{2-}$, $[Fe_2(SR)_6]^{2-}$ or $[Fe_4(SR)_{10}]^{2-}$ are important steps in the reaction. Similar reactions occur when Se is used instead of S [18].

Elemental iron has also been used as the metal source. In this case, both S and I_2 can oxidize the metal [52,80].

$$6Fe + 6S + 2I_2 + 2I^- \rightarrow [Fe_6S_6I_6]^{2-}\,(\mathbf{10})$$

$$4Fe(CO)_5 + 4S + I_2 + 2I^- \rightarrow [Fe_4S_4I_4]^{2-}\,(\mathbf{7}) + 20CO$$

(2) Chalcogenides, E^{2-}, as chalcogen source. Replacing chalcogens with chalcogenide anions in the reactions shown in the previous section yielded a large variety of clusters. Some representative reactions are shown in Scheme 3.

Triangular capped complexes, **3**, are obtained through the simple metathetical reaction (1) of Scheme 3 [20].

Redox processes are in turn involved in the synthesis of tetra- and hexa-metallic iron clusters (reactions (2)–(7)). In reactions (2) [81] and (3) [82], the iron(III) is reduced by SR^- and by S^{2-} respectively, while the stoichiometries of the other reactions are still unclear. The synthesis of the cubane-like reduced core $[Fe_4Te_4]^+$ might be due to the high redox power of telluride solutions (reaction (4)) [30].

It is interesting to note again that similar reaction systems $FeCl_3/S^{2-}/SR^-$ but

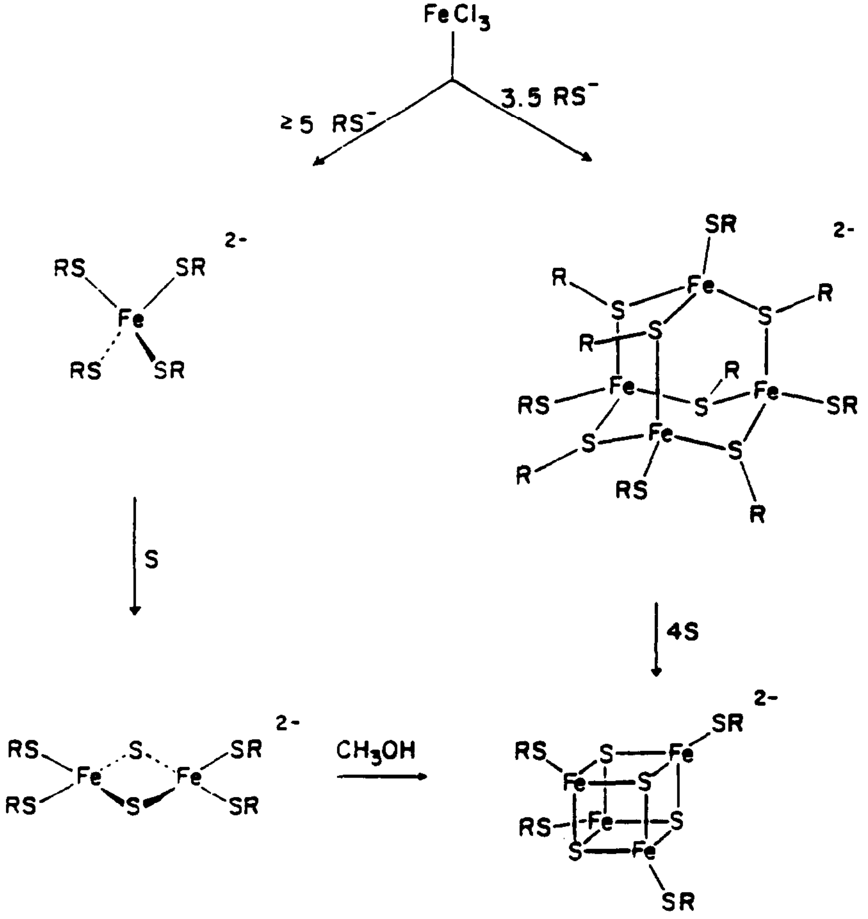

Scheme 1. (From ref. 75.)

with different reagent ratios (reactions (2) and (5)) afford different clusters [56]. The uncharged phosphine ligands, PEt_3, favour the formation of basket-like clusters (reactions (6) and (7)) [53,55].

Finally, it has recently been found that direct reactions of $FeCl_3$ with E^{2-} in the presence of weak ligands such as $[PhNC(O)Me]^-$ provide high nuclearity exotic clusters, without terminal ligands, such as $[Na_2Fe_{18}S_{30}]^{8-}$ [72] and $[Na_9Fe_{20}Se_{38}]^{9-}$ [73].

(3) Hydrogen chalcogenides ions, EH^-, as chalcogen source. The use of EH^- as chalcogen source allows the formation of different clusters (Tables 1 and 2). Some representative reactions are collected in Scheme 4. The first reported synthesis of an iron–sulphur cubane-like cluster used SH^- ions as sulphur source according to reaction (1) of Scheme 4 [32]. In this reaction, SR^- is acting as the reducing agent

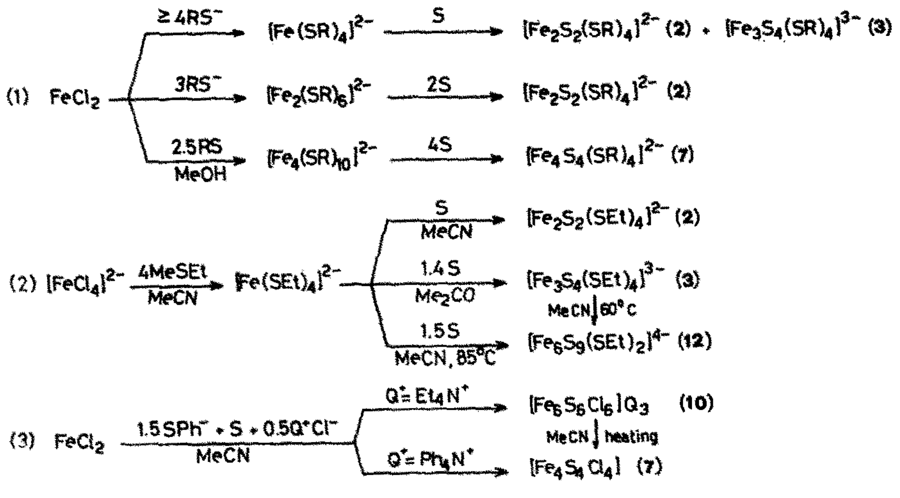

Scheme 2.

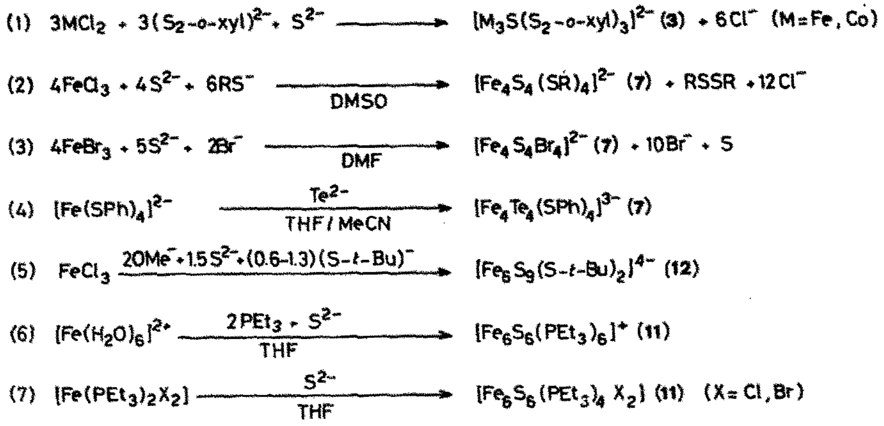

Scheme 3.

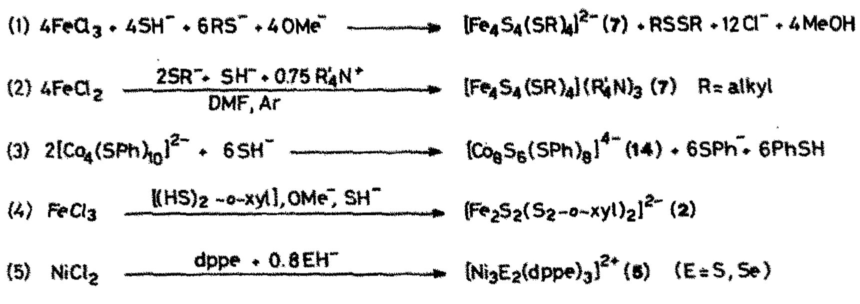

Scheme 4.

of iron(III). Similar reactions occur with SeH^- [33]. Quite interestingly, the related $FeCl_2/SR^-/SH^-$ system permits the direct synthesis of the $[Fe_4S_4(SR)_4]^{3-}$ species containing the reduced core $[Fe_4S_4]^+$ (reaction (2), [83]. This reaction probably occurs via the formation of the adamantane-like cage complex $[Fe_4(SEt)_{10}]^{2-}$, but the actual oxidant of iron(II) remains unidentified.

Reactions (3) [62], (4) [10], and (5) [84] do not involve either reduction or oxidation of the metals.

(4) Dihydrogen chalcogenides, H_2E, as chalcogen source. It was generally recognized 25 years ago that the reactions of divalent 3d metal ions with H_2S invariably afforded insoluble binary sulphides. However, Sacconi and coworkers found that iron(II), cobalt(II) and nickel(II) salts, in the presence of tertiary phosphine ligands, reacted with H_2S to yield soluble mercapto- and thio-derivatives [11,85]. Typical reactions affording metal–chalcogen clusters are shown in Scheme 5. Whereas, in the presence of the tridentate ligand triphos, only dimetallic species were isolated (reaction (1) of Scheme 5) [11,15], triethylphosphine permits the synthesis of tri-, hexa-, and nona-metallic clusters (reactions (2) [43,45,86], and (3) [23,67]. Reactions (1) and (3) also occur using H_2Se or H_2Te in place of H_2S, but in this case reaction (3) only affords the trimetallic species **5** [24,25,87]. In reactions (4) [26] and (5) [37], low-valent metal species have been used as metal sources. Apart from complexes of structural types **1** and **5**, the formation of the clusters involves partial or complete oxidation of the metal. The mechanism of these reactions is still unclear. Two possible pathways which permit the formation of M–S–M bridges, with oxidation of the metal ions, can likely be proposed (Scheme 6). In both cases, the first step is coordination of H_2S to the metal centre: in case (1), the rapid formation of a mercapto derivative, in presence of a base B, is followed by elimination of H_2; in case (2), oxidative addition of H_2S to the metal occurs with formation of a mercaptohydride and subsequent elimination of H_2. The formal oxidation state of the metal is increased

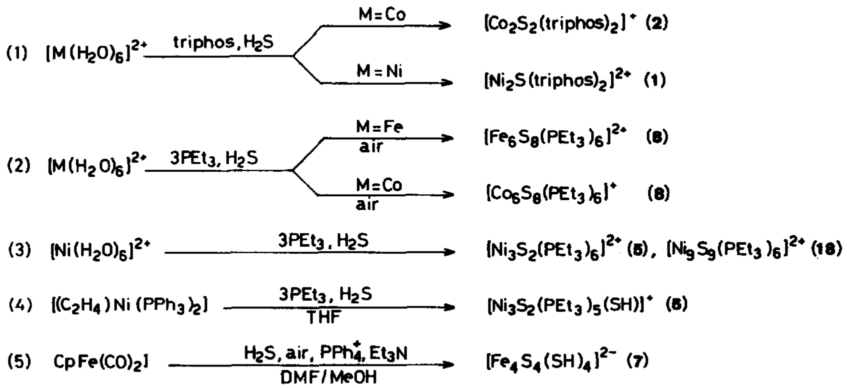

Scheme 5.

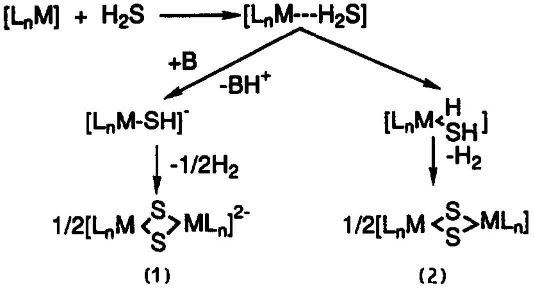

Scheme 6.

by 1 and 2, respectively. Formation of SH complexes of 3d metal ions by reaction with H_2S, in the presence of a base, is well documented (reaction (1) of Scheme 7 [88]). Oxidative addition of H_2S to a metal centre followed by subsequent H_2 elimination has recently been reported for a rhodium complex with a tripod-like ligand (reaction (2) of Scheme 7) [89].

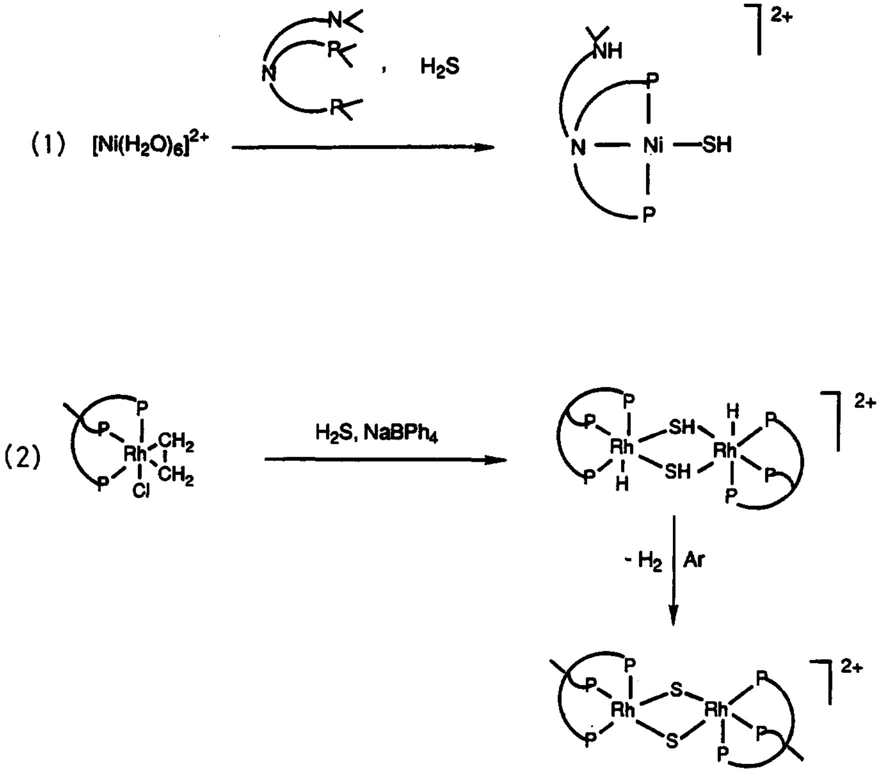

Scheme 7.

(5) $E(SiMe_3)_2$ as chalcogen source. This particular type of self-assembly reaction was principally developed by Fenske et al. [9]. Some typical reactions are shown in Scheme 8; reactions (1) and (4) are described in refs. 59 and 90. Generally, halide–monotertiary phosphine–metal(II) complex reacts, in organic solvents, with $E(SiMe_3)_2$. A great variety of clusters, many of them with high nuclearity, were obtained in this way depending on the ratio $M:E:PR_3$, the solvent (usually toluene, MeCN, THF), the nature of PR_3, and the nature of the halide. The formation of uncharged species appears highly favoured. The breaking of the M–X and E–Si bonds with formation of $XSiR_3$ and M–E bonds are obvious steps in these reactions. However, the redox processes which occur and also the general stoichiometries remain unclear. This method allowed the preparation of $[Co_6S_4I_2(PEt_3)_6]^{2+}$, a unique cluster containing bridging S and I atoms in the inner core. The structure of this cluster is shown in Fig. 17 [90].

(6) Miscellaneous sources of chalcogens. Organic trisulphides, R–S–S–S–R, have been used successfully as sulphur sources in place of elemental sulphur in reactions similar to those described in Sect. B. (ii)(a)(1) (reaction (1) of Scheme 9) [91], whereas solutions of polysulphides or polyselenides can act as sources of chalcogens in the assembly of hexametallic iron clusters (reaction (2)) [57,58].

Steigerwald et al. [47,66] have recently found that the labile adduct $TePEt_3$ is an efficient source of tellurium for the synthesis of high-nuclearity of metal–tellurium clusters (reactions (3) and (4)).

(b) Redox reactions

A basic function of the metal–sulphur clusters found in living organisms is their behaviour as electron carriers in redox processes. The electrochemical behaviour of

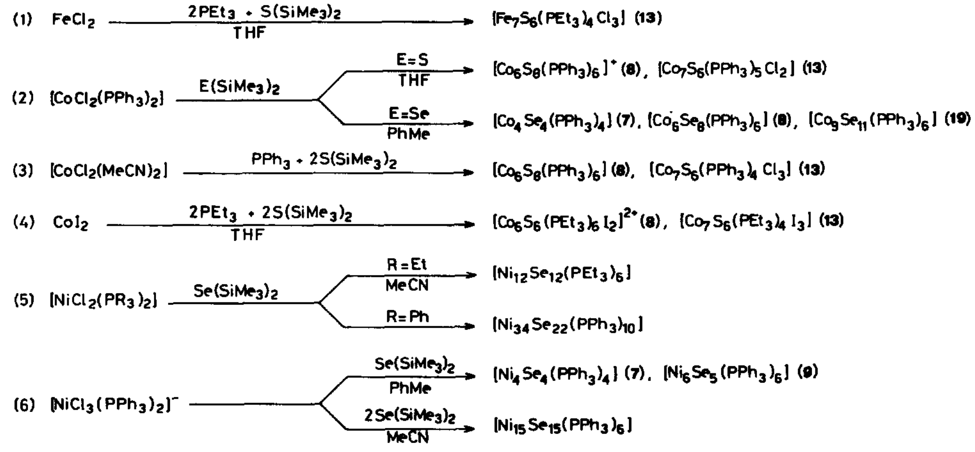

Scheme 8.

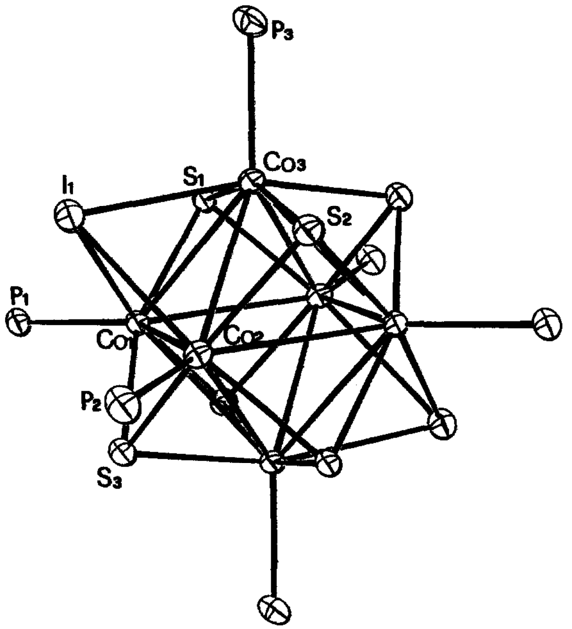

Fig. 17. Perspective view of $[Co_6S_6I_2(PEt_3)_6]^{2+}$. (From ref. 90.)

the synthetic clusters was carefully studied and recently reviewed [92]. The oxidation or reduction of a cluster is a straightforward method to prepare species with similar geometries but different oxidation states. As a matter of fact, clusters belonging to the structural types **2**, **7**, **8**, **10** and **14** undergo redox processes under mild conditions. Sodium tetrahydroborate [15], sodium naphthalenide [15], sodium acenaphthylenide [29,62], nitrosyl tetrafluoroborate [15] and ferrocinium tetrafluoroborate [40] have been used in turn as reducing or oxidizing agents, respectively. It is noteworthy that these clusters contain highly symmetric cores in which all the metals are nearly equivalent.

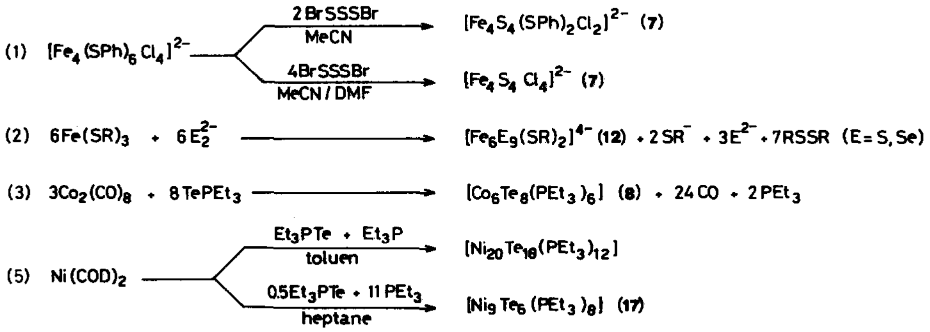

$$(1)\quad [Fe_4(SPh)_6Cl_4]^{2-} \xrightarrow[MeCN]{2BrSSSBr} [Fe_4S_4(SPh)_2Cl_2]^{2-}\ (7)$$

$$[Fe_4(SPh)_6Cl_4]^{2-} \xrightarrow[MeCN/DMF]{4BrSSSBr} [Fe_4S_4Cl_4]^{2-}\ (7)$$

$$(2)\quad 6Fe(SR)_3 + 6E_2^{2-} \longrightarrow [Fe_6E_9(SR)_2]^{4-}\ (12) + 2SR^- + 3E^{2-} + 7RSSR\ (E = S, Se)$$

$$(3)\quad 3Co_2(CO)_8 + 8TePEt_3 \longrightarrow [Co_6Te_8(PEt_3)_6]\ (8) + 24CO + 2PEt_3$$

$$(5)\quad Ni(COD)_2 \xrightarrow[toluen]{Et_3PTe + Et_3P} [Ni_{20}Te_{18}(PEt_3)_{12}]$$

$$Ni(COD)_2 \xrightarrow[heptane]{0.5Et_3PTe + 11PEt_3} [Ni_9Te_6(PEt_3)_8]\ (17)$$

Scheme 9.

(c) Coupling reactions

The reaction of a metal–chalcogen cluster with an elemental metal, a metal complex, or another cluster can afford new clusters with different nuclearity as appears in Scheme 10. The cuboidal cluster $[Fe_8S_6I_8]^{3-}$ was obtained by capping the open faces of the prisman-like $[Fe_6S_6I_6]^{2-}$ ion, using Fe metal, I^-, and I_2 (reaction (1) of Scheme 10) [61]. Reactions (2) are models for incubations of proteins having cuboidal Fe_3S_4 cores with M^{2+} salts [41].

Using topological considerations, Feske et al. [9] suggested that aggregation to more highly condensed compounds by the reactions of Sect. B. (ii)(a)(5) occurred via smaller fragments. In this framework, the trimetallic units **5** should be the structural units to assemble cluster cores **8**, **18** and **19**.

(d) Terminal ligand exchange reactions

Ligand substitution is a fundamental process in the chemistry of synthetic iron–sulphur clusters. Indeed, this reaction forms the basis of the core extrusion method [93], useful for identifying some clusters present in proteins, and allows the introduction of diverse chemical environments around the iron–sulphur core. These reactions concern essentially iron clusters of types **2** and **7**.

The most straightforward substitution method is to react the chalcolgenide ligated species with the sodium salt of an anionic ligand, the precipitation of NaCl driving the reaction to completion as in reaction (1) of Scheme 11.

Thiolate ligand substitution reaction (2) occurs via stepwise reversible equilibria. The reaction proceeds to the right provided that the acidity of R′SH is stronger than that of RSH [94].

Ligand substitution can likewise be affected with electrophilic reagents EL with E = H, acyl, sulphoxyl, and L = halide, thiolate, phenolate, carboxylate, etc. (reaction (4)) [36,95].

A fundamental characteristic of these reactions is that they give rise to a statistical mixture of products which can occasionally be differentiated only in the solid state. The independent reactivity of the terminal ligands is due to the fact that they are separated by 6–7 Å around a nearly dimensionally isotropic cluster core.

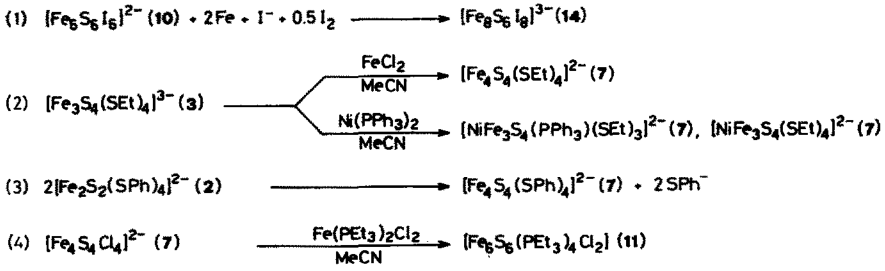

Scheme 10.

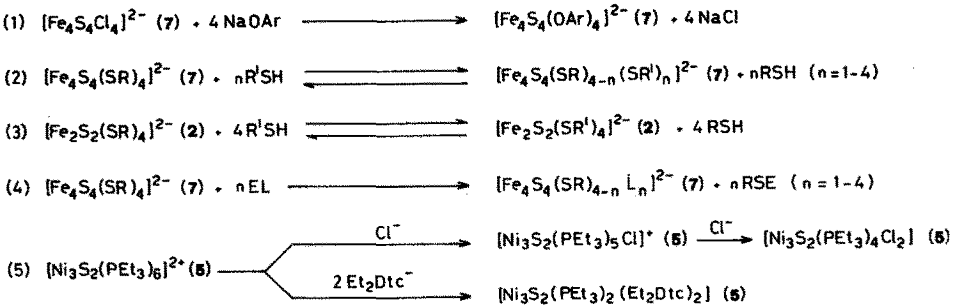

Scheme 11.

Recently, Holm et al. have synthesized cubane-type clusters of formula $[Fe_4S_4(LS_3)L']^{2-}$ (LS_3 is a semi-rigid tridentate thiolate ligand) (Fig. 18) containing core units whose iron subsites are differentiated in the ratio 3:1 [39,96]. In this way, they skilfully solved the problem of performing site-specific chemistry at one iron site in a Fe_4S_4 cluster.

Terminal ligand substitution reactions have also been carried out on type **5** nickel clusters (reaction (5) of Scheme 11). In this case, only the synthesis of differentiated subsites was achieved [25,27].

C. ELECTRONIC STRUCTURE OF PARAMAGNETIC CLUSTERS

(i) Weak bonding: the exchange interaction

Usually, the formation of a covalent bond in molecules results in an antiparallel alignment of the electronic spins in a molecular orbital, unless a system with an odd number of electrons is considered or some orbital degeneracy is present. States with a total spin different from that of the ground state are at energies much higher than kT when T is room temperature. In polynuclear transition metal complexes, especially those with metals of the first transition series, the metal atoms are separated by intervening ligands, but the metals in the complex do not behave independently. For example, in dinuclear copper(II) complexes with oxalato moieties as bridging units [97], in which the metals are more than 500 pm apart, the electrons on the metal centres are correlated and the magnetic moment of the complex is temperature dependent because the splitting between the singlet and triplet spin states, $\Delta E \approx 390\ \mathrm{cm}^{-1}$, is comparable with kT. As a consequence, the bonding interactions in polynuclear transition metal complexes cannot easily be rationalized using a molecular orbital scheme and are generally called "weak-bonding" interactions. Their theoretical treatment requires the use of configuration interactions calculations and a phenomenological approach is widely used by experimentalists to rationalize the experimental properties of polynuclear complexes. In this approach, the multiplet

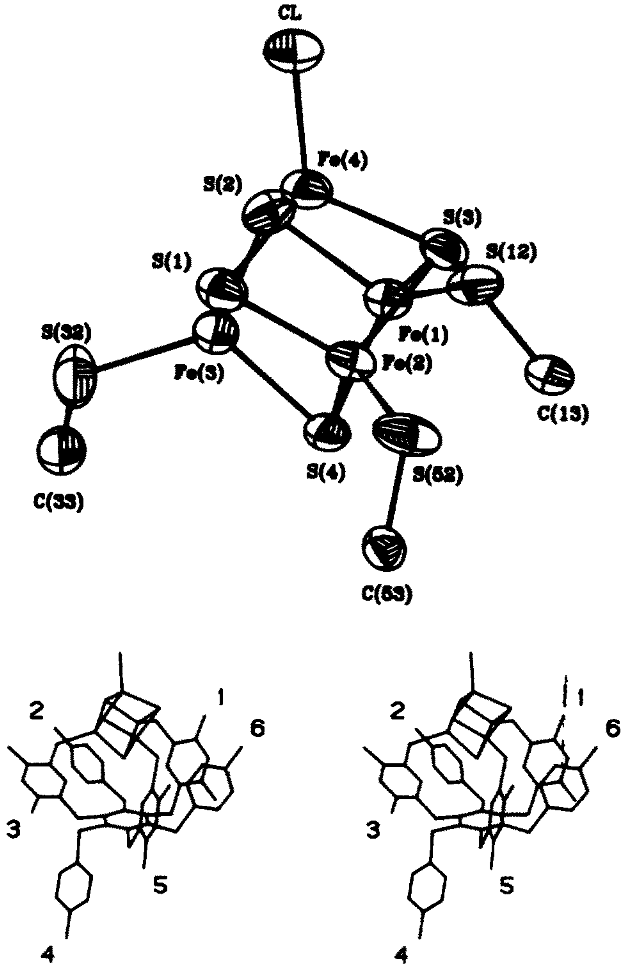

Fig. 18. Structure of $[Fe_4S_4(LS_3)Cl]^{2-}$. Above: ORTEP view of the skeleton. Below: stereoview of the entire structure. (From ref. 39.)

structure is derived as a consequence of a magnetic coupling between the spins of the interacting metal ions through a spin hamiltonian [98], which allows one to parameterize the relative energies of the various multiplets; this is called the exchange spin hamiltonian. The theoretical models will therefore be concerned with the correlation between the spin hamiltonian parameters and the electronic and geometrical structure of the polynuclear compound [99].

A common form of the spin hamiltonian used to describe the interaction between two magnetic centres is

$$H = J\mathbf{S}_1 \cdot \mathbf{S}_2 + \mathbf{S}_1 \cdot \mathbf{D}_{12} \cdot \mathbf{S}_2 + \mathbf{d}_{12} \cdot \mathbf{S}_1 \times \mathbf{S}_2 \qquad (1)$$

where the first term accounts for the isotropic exchange interaction, which can be directly linked to the weak-bonding interaction, and the other terms, the anisotropic and the antisymmetric interactions, originate from direct magnetic interactions and spin orbit coupling effects. Usually, the values of J are of the order of hundreds of wavenumbers, while D_{12} rarely exceeds few wavenumbers and d_{12} is smaller. J_{12} can thus describe the overall ordering of the spin states in a large number of cases.

In the dinuclear case, the spin states arising from the exchange interaction can be conveniently labelled using the total spin quantum numbers, S, arising from the vector coupling of the $\mathbf{S}_1$ and $\mathbf{S}_2$ spin operators. S must obey the equation

$$|S_1 - S_2| \leqslant S \leqslant S_1 + S_2 \tag{2}$$

the relative energies of the spin states are thus given by

$$E(S) - E(S-1) = JS \tag{3}$$

In the case of dinuclear compounds with only two unpaired electrons, $S_1 = S_2 = 1/2$, S can be 0 or 1 and J represents the separation between the triplet and the singlet states. The other terms in eqn. (1) remove the degeneracy of the M_S levels of each S manifold. The J values can conveniently be obtained by measuring the temperature dependence of the magnetic susceptibility, the effects of the anisotropic interactions can be observed through EPR spectroscopy, while the effects of the antisymmetric interaction are most subtle and are more difficult to ascertain. A recent book by Bencini and Gatteschi [100] exploits most of the subtleties of the spin hamiltonian of eqn. (1), reviews the application of the EPR spectroscopy to the characterization of the magnetic structure in polynuclear compounds, and collects the results of the Florence group in the field.

Quite often, one single technique is not able to describe completely the magnetic structure of a cluster. A nice example [101] is given by the complex of formula $\mathrm{Cu(salen)Ni(hfa)_2}$ shown in Fig. 19. Magnetic susceptibility studies showed that the copper(II), $S_{\mathrm{Cu}} = 1/2$, and the nickel(II), $S_{\mathrm{Ni}} = 1$, ions are antiferromagnetically coupled to yield an $S = 1/2$ ground state. The single crystal EPR spectra were, however, characteristic of a triplet species split in zero field by $|D| = 3|D_{zz}|/2 = 0.12\ \mathrm{cm^{-1}}$ and $E = (D_{xx} - D_{yy})/2 = 0.019\ \mathrm{cm^{-1}}$. This triplet state was found to arise from the interaction between two molecular units which in the solid state are in close contact. The combined use of EPR and magnetic techniques gave the spin level structure shown in Fig. 20.

NMR spectroscopy has been applied to investigate the electronic structure of paramagnetic metal clusters in proteins and these applications have recently been reviewed [102].

(a) Semiempirical models of the exchange interaction

In 1963, Anderson [103] completed the formulation of the first theory of the exchange interaction. Considering a pair of interacting centres A and B with one unpaired electron on each centre and orbitally non-degenerate ground states, the

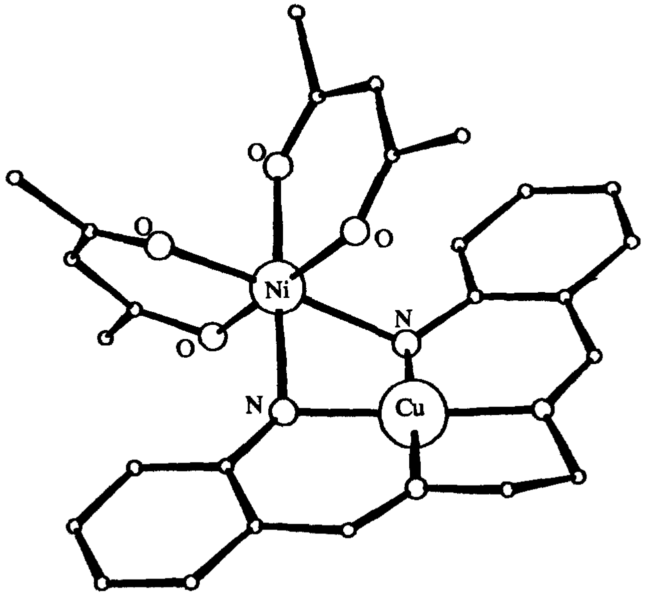

Fig. 19. Structure of Cu(salen)Ni(hfa)$_2$.

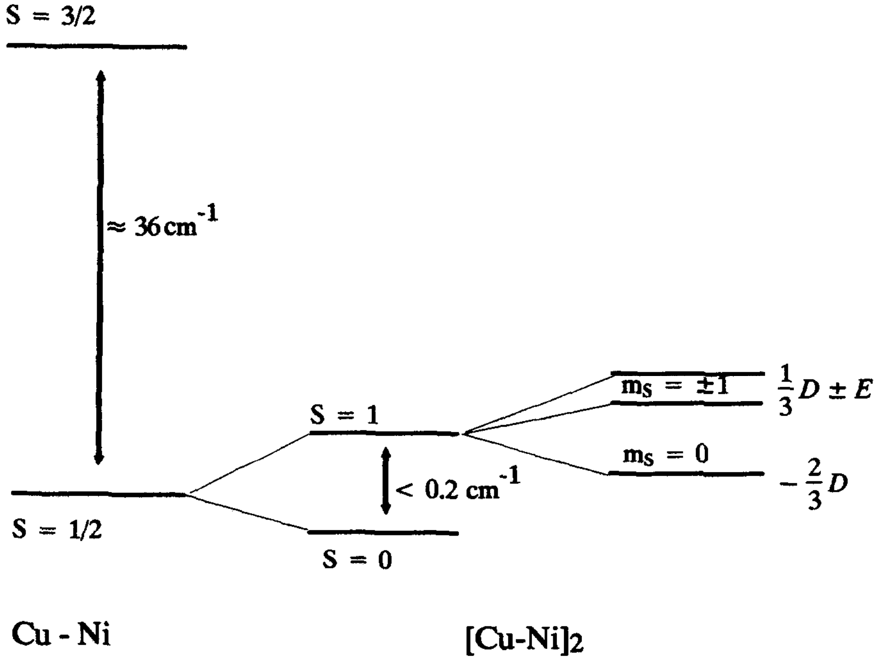

Fig. 20. Spin level structure of the copper–nickel pairs in Cu(salen)Ni(hfa)$_2$.

ground state of the whole system can be represented using an antisymmetrized product of functions localized on the two centres (magnetic orbitals). When these orbitals are allowed to interact, we have a partial delocalization of the electron on A onto centre B and vice versa. This means that ionic configurations of the type A^+B^- and A^-B^+ must contribute to the ground state. Since these ionic configurations are necessarily singlet states, the singlet state of the system is stabilized by an energy

$$\Delta E = \frac{2b_{AB}^2}{U} \tag{4}$$

where b_{AB} is the transfer integral between the magnetic orbital on A and that on B and U is the energy of the ionic states with respect to the covalent state. This term is called *kinetic exchange.* A second contribution must be taken into consideration arising from the self-energy of the charge distribution $\rho_{AB} = \phi_A^* \phi_B$ and is given by the exchange integral

$$K_{AB} = \int \phi_A^*(1)\phi_B^*(2)e^2/r_{12}\phi_A(2)\phi_B(1)\,d\tau \tag{5}$$

where ϕ_A and ϕ_B are the magnetic orbitals on A and B, respectively. This term, called *potential exchange*, stabilizes the triplet state. The overall exchange interaction then takes the form

$$E(S=1) - E(S=0) = J = \frac{2b_{AB}^2}{U} - K_{AB} \tag{6}$$

This rationalization of the exchange interaction allowed Goodenough and Kanamori [104,105] to express some practical rules which allowed the experimentalists to correlate the sign of the exchange interaction to the topology of the magnetic orbitals.

The quantitative applications of eqn. (6) were found to be practically impossible and Anderson himself stated: "it seems wise not to claim better than about 100% accuracy for the theory in view of uncertainties" (i.e. the error can be 100%!). In 1975, Hay et al. [106] showed that, including configuration interaction at the second order in perturbation theory, the singlet–triplet separation, J, can be written as

$$E(S=1) - E(S=0) = J = -2K_{AB} + \frac{(\varepsilon_u - \varepsilon_g)^2}{(J_{AA} - J_{AB})} \tag{7}$$

where K_{AB} and J_{AA} and J_{AB} are the exchange and Coulomb integrals between the magnetic orbitals localized on centres A and B, respectively. In their procedure, the magnetic orbitals are obtained from the localization of the molecular orbitals computed from an MO-SCF calculation on the triplet state as

$$\phi_A = \frac{[\phi_g + \phi_u]}{2}; \quad \phi_B = \frac{[\phi_g - \phi_u]}{2} \tag{8}$$

where ϕ_g and ϕ_u are the two singly occupied molecular orbitals of the triplet state, with energies ε_g and ε_u. Since the magnetic orbitals in eqn. (8) are orthogonal to each other, K_{AB} is always positive and eqn. (7) can be rewritten as

$$J = J_F + J_{AF} \tag{9}$$

where J_F is a negative term which favours the stabilization of the triplet state (ferromagnetic contribution) and J_{AF} is a positive term which stabilizes the singlet state (antiferromagnetic contribution). Equation (7) strongly resembles eqn. (6), but the antiferromagnetic term can now be computed through a molecular orbital calculation. An equation similar to eqn. (9) was developed by Kahn and Briat [107] in 1976 using non-orthogonal magnetic orbitals.

The advantage of eqn. (7) over eqn. (6) is that, if one is dealing with a series of complexes in which the ferromagnetic term can be considered as a constant, the energy difference $\varepsilon_u - \varepsilon_g$ is responsible for the variation of J and eqn. (7), in this approximation, was indeed successfully used to correlate observed variations of J to bonding and geometrical features. As examples of applications, we now consider μ-chloro- and μ-carbonato-bridged copper(II) dimers shown in Fig. 21. In the μ-chloro complexes, the copper ions are in a square planar coordination environment when the angle $\phi = 0°$ and in a pseudotetrahedral coordination for $\phi = 90°$. All the experimental systems were found to possess ϕ angles ranging between 0° and 45°. Experimentally, a net antiferromagnetic coupling results when ϕ is close to 0°, while a ferromagnetic interaction is operative when ϕ approaches 45°. In μ-carbonato bridged dimers the symmetric dimers with $\alpha = 90°$ were found to be diamagnetic and those with $\alpha > 90°$ were found to be antiferromagnetically coupled. Extended Hückel calculations [106,108] showed that, in both cases, the singly occupied molecular orbitals are linear combinations of mainly d_{xy} atomic orbitals of copper. The variation of their energies as a function of the ϕ and α geometrical parameters for the μ-chloro and μ-carbonato bridged complexes, respectively, are shown in Fig. 22. In the first

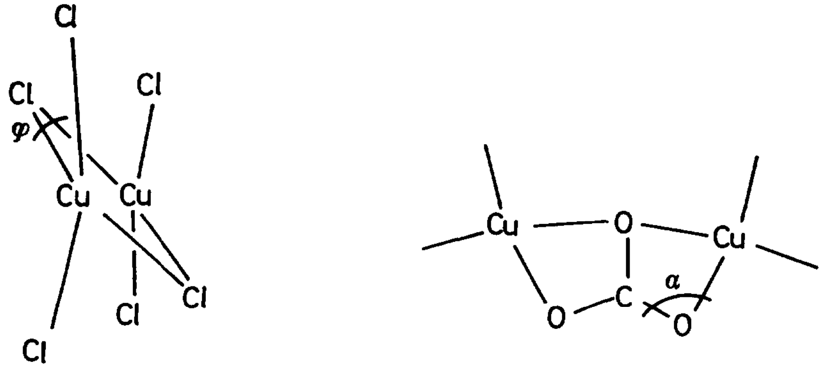

Fig. 21. Schematic view of the $[Cu_2Cl_6]^{2-}$ ion and of the core of dinuclear μ-carbonato-bridged copper(II) complexes.

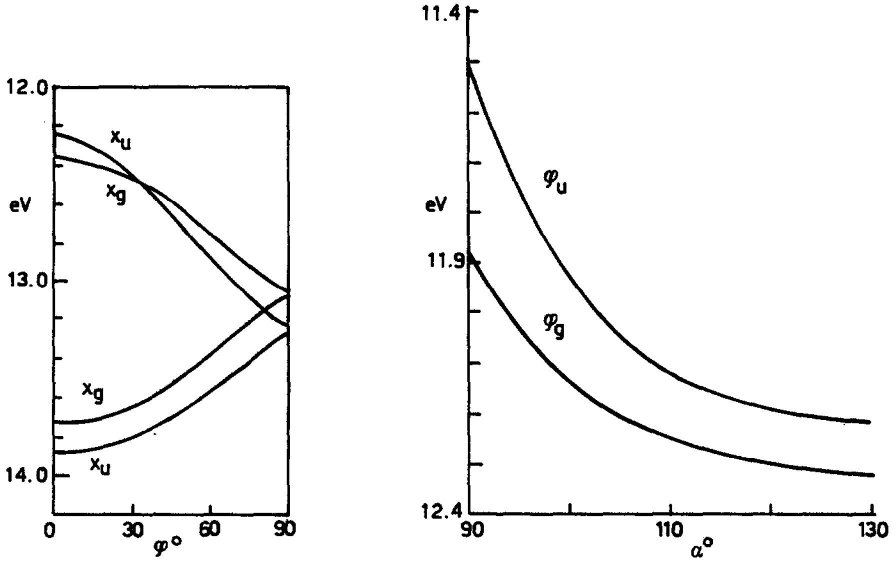

Fig. 22. The energies of the highest occupied molecular orbitals for μ-chloro (left) and μ-carbonato-bridged (right) copper(II) complexes computed by extended Hückel calculations for different values of ϕ and α. (From refs. 106 and 108.)

case, a crossing of levels occurs (computed around 30°) and around this value the J_F term is anticipated to be dominant in eqn. (9). On proceeding towards 90°, the energy separation increases and an antiferromagnetic contribution is anticipated. Unfortunately, so far no compounds with ϕ larger than 45° have been synthesized. For the μ-carbonato bridged dimers, no crossing of levels is computed, thus explaining the experimental observations which locate the singlet at lower energy than the triplet. A larger energy separation is computed for $\alpha = 90°$, thus qualitatively explaining the observed diamagnetism of the compounds.

The above model can easily be extended to dinuclear units with more than two interacting electrons, the overall interaction being, in this case, reduced to a sum of interactions between pairs of molecular orbitals [106].

Similar qualitative arguments have been used to correlate magnetic and structural properties in dinuclear complexes with bridging alkoxo [106,109,110], pyrazolato [111], azido [109,112], oxalato, oxamidato and related ligands [113] and chalcogenides groups [68,114].

The extension of the above model to clusters with nuclearity larger than two is not straightforward and the number of geometrical parameters to be considered increases. As a matter of fact, no application has been reported so far except for cases in which the dominant interactions involve pairs of transition metals. Furthermore, when tetra, hexa, and higher nuclearity clusters are concerned, the interest of the researchers has so far been focused mainly on electron transfer properties and

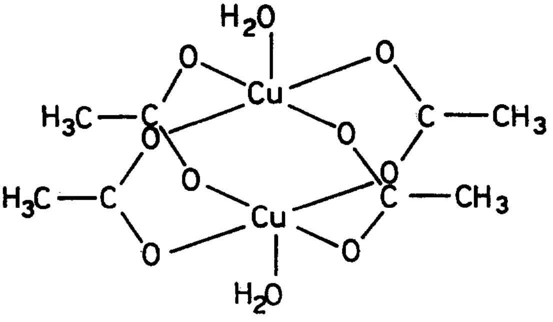

Fig. 23. Structure of copper(II) acetate hydrate.

the magnetic behaviour of these clusters was generally reported without any further comment.

(b) Quantitative calculations of the exchange coupling constants

In 1981, de Loth et al. [115] reported the first successful quantitative calculations of singlet–triplet separation in a transition metal dimer. The complex chosen was the copper acetate hydrate sketched in Fig. 23. The authors showed that the singlet–triplet energy difference can be expanded in series using a perturbative development of the configuration interaction problem. This is, in a sense, a further development of the Hay et al. model [106] which appears in this framework to be corrected at second order. The CI problem was then treated at the ab initio level using a pseudopotential approach and the results for the copper acetate hydrate are summarized in Fig. 24. The computed value of the singlet–triplet splitting is 245 cm^{-1} with the singlet at lower energy. This is in nice agreement with experience, which shows

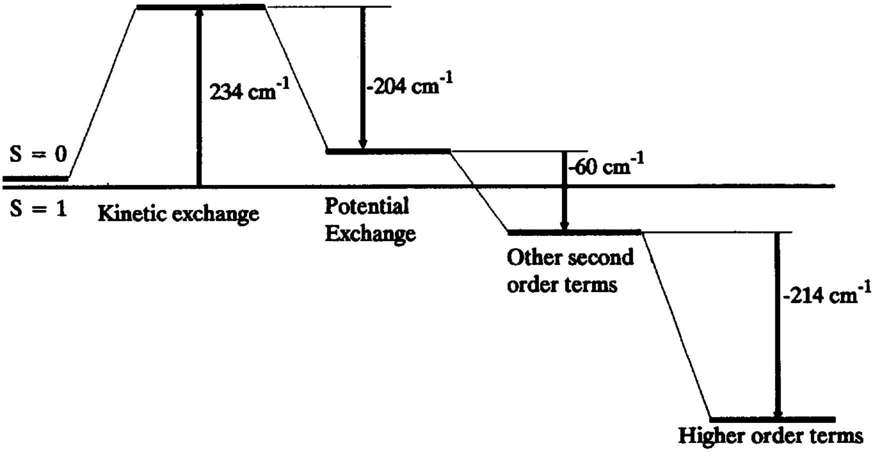

Fig. 24. Results of ab initio calculation of the singlet–triplet splitting in copper(II) acetate hydrate. (From ref. 115.)

that the triplet state is $\approx 290\ \text{cm}^{-1}$ above the singlet state. This result is obtained only after inclusion of higher-order perturbation terms. The ferromagnetic term, which is related to the potential exchange in the Anderson theory [103], is a very important factor. The same model has been successfully applied to the calculation of the singlet–triplet splitting in dinuclear copper(II) complexes with hydroxo [116], azido [116], and oxalato-like [116,117] bridging groups and to the calculation of the singlet–triplet splitting in a copper(II)–vanadyl(IV) complex exhibiting a ferromagnetic ground state [118]. The influence of the calculation ingredients on the final value of J, like the choice of the atomic basis set and the ligand model, has been studied in a variety of cases [117,119–122]. Direct calculations of the singlet–triplet splitting on model systems using other ab initio methodologies have also been performed [123] and a VB approach has been applied to the calculation of the singlet–triplet splitting in copper acetate [124].

In 1979, Noodleman and Norman [125] developed a formalism particularly well suited for density functional theories [126] to compute the magnetic structure of dinuclear compounds. The basis of the method is the construction of a Slater determinant of broken spin and space symmetry. This determinant is built up using basis functions which are symmetry adapted to a subgroup of the full molecular point group, in particular any symmetry element relating to the two metal centres of the dinuclear unit is removed. Later, a specular symmetry is imposed on the spin densities of the two halves of the molecule. This procedure leads to a localization of the molecular orbitals and the unpaired electrons are in overlapping magnetic orbitals localized onto different parts of the molecule [127]. The extent of localization depends on the overlap: small overlap means weak bonding interaction and good localization of the magnetic orbitals. Considering, for the sake of simplicity, the case of two magnetic orbitals and two unpaired electrons, the energy of this broken symmetry determinant, $|b\rangle$, which corresponds to a spin state with $M_S = 0$, can be expressed through the energies of the singlet and triplet states as

$$E_b = \frac{[E(S=0) + RE(S=1)]}{(1+R)^{-1}} \tag{10}$$

where

$$R = \frac{(1 - S_{AB}^2)}{(1 + S_{AB}^2)} \tag{11}$$

and S_{AB} is the overlap integral between the magnetic orbitals. For weakly interacting dimers, $S_{AB}^2 < 1$ ($R \approx 1$) and eqn. (10) becomes [127]

$$E_b \approx \frac{[E(S=0) + E(S=1)]}{2} \tag{12}$$

Comparing eqn. (12) with the isotropic part of the spin hamiltonian of eqn. (1), we obtain the fundamental equation

$$J = 2[E(S=1) - E_b] \tag{13}$$

When the bonding interaction is not weak, we are in the limit of strong overlap between the magnetic orbitals, $S_{AB} \approx 1$, and $R \approx 0$. In this case, eqn. (10) becomes

$$Eb \approx E(S=0) \tag{14}$$

and we have

$$J = E(S=1) - Eb \tag{15}$$

The exact value of J in the general case will be intermediate between eqns. (13) and (15).

Let us now show two examples of the above model. The systems chosen are the $[Cu_2Cl_6]^{2-}$ and the μ-carbonato-bridged copper(II) dimers whose magnetic properties have been qualitatively investigated in Sect. C.(i).

In Fig. 25, a contour map of the magnetic orbitals computed for $[Cu_2Cl_6]^{2-}$ for $\phi = 0°$ and $\phi = 45°$, using the Xα-SW method [128,129], is shown [130]. It is

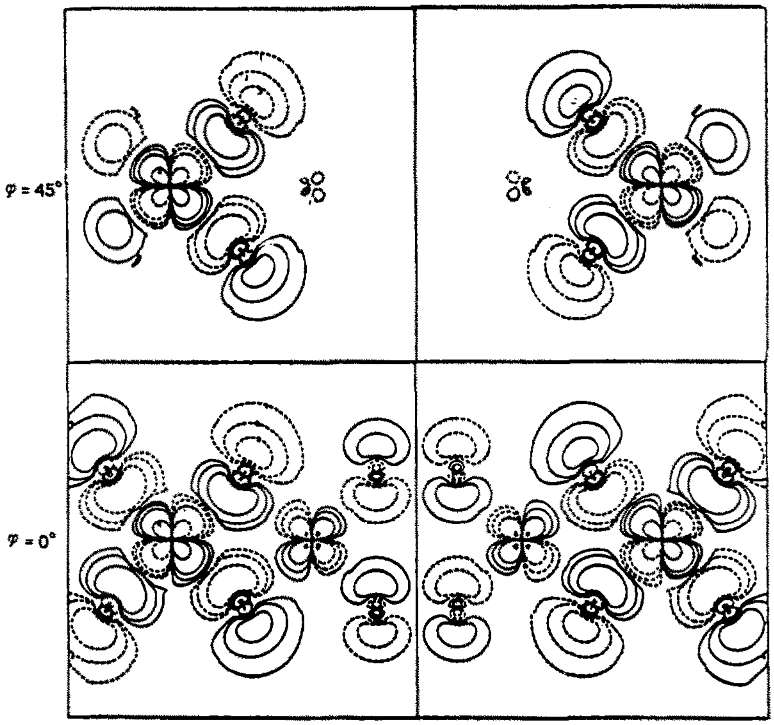

Fig. 25. Contour maps of the magnetic orbitals of $[Cu_2Cl_6]^{2-}$ obtained from Xα-SW calculations. Spin up levels are plotted on the left, spin down levels are plotted on the right. Dotted lines represent negative values. (From ref. 128.)

TABLE 3

Observed and computed J values for $[Cu_2Ci_6]^{2-}$ dimers[a]

Compound	ϕ (deg)	J_0 (cm^{-1})	J_C (cm^{-1})
$[LiCuCl_3]_2 \cdot 2H_2O$	0	>0	197.6
$[KCuCl_3]_2$	0	40	
$[Me_2NH_2CuCl_3]_2$	0	3	
$[(Ph_4Sb)CuCl_3]_2$	44.4	−90	
	45.0		−210
$[(Ph_4As)CuCl_3]_2$	48.2	−80	
$[(Ph_4P)CuCl_3]_2$	50	−80	

[a] Details on the method of calculations are given in ref. 128.

apparent that for $\phi = 45°$ the magnetic orbitals are largely localized onto the metals and the overlap between them is smaller than for the planar case, qualitatively justifying the computed and observed ferromagnetism. The computed values of J are compared with the experimental figures in Table 3. The overall agreement with experiment, as far as the order of magnitude and the sign of the interaction is concerned, is apparent. Of course, in these types of calculation, complete numerical agreement with experimental J values is not found since it is actually dependent on the details of the real geometrical structure of the systems.

An opposite situation is encountered for the μ-carbonato complex $[Cl_3Cu(CO_3)CuCl_3]^{4-}$, which was used to model the experimentally obtained complexes [108]. The contour maps of the magnetic orbitals, computed through Xα-SW calculations, are shown in Fig. 26. It is apparent that the extent of localization is much smaller than in the previous examples, indicating a stronger bonding interaction and justifying the observed diamagnetism of the complexes actually synthesized. The value of J calculated using eqn. (15) is in this case, 4710 cm^{-1}. Although this value cannot be measured experimentally, it provides a theoretical interpretation of the diamagnetism observed in the real systems. Other examples of the application of the method are to copper(II) dimers with a μ-oxo bridge [131], to a copper(II)–vanadyl(IV) complex [132], and to dinuclear iron–sulphur complexes [133–135].

The above model can quite easily be extended to calculations of the magnetic structure of more complex systems. Examples of the application of the model to the calculation of the magnetic structure of iron–sulphur clusters are reported in refs. 135–138.

It must be stressed at the end of this section how the proposed theoretical tools differ substantially in their essence. The semiempirical models allow one to draw qualitative magneto-structural correlations; the ab initio models give J values which are in extremely good agreement with the experimental values, even if they required a long CI procedure and there are no general criteria which allow one to predict

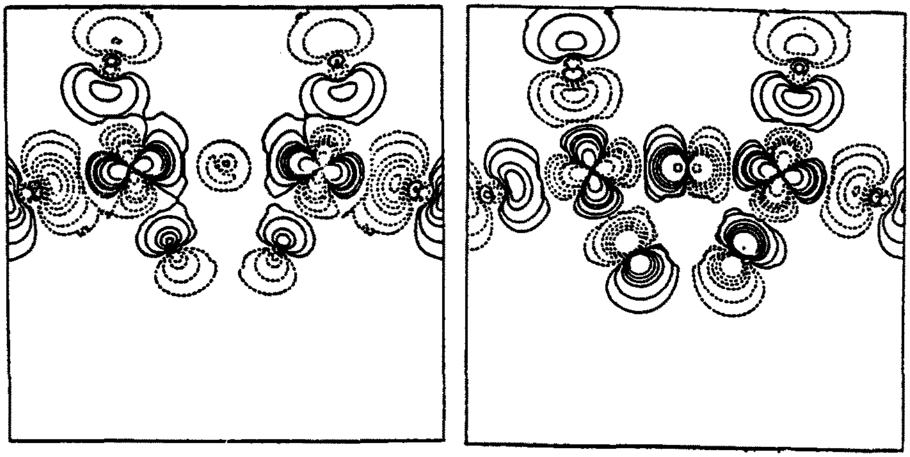

Fig. 26. Contour maps of the magnetic orbitals of $[Cl_3Cu(CO_3)Cl_3]^{4-}$ obtained from Xα-SW calculations. Spin up levels are plotted on the left, spin down levels are plotted on the right. Dotted lines represent negative values. (From ref. 108.)

where to stop the perturbation procedure; furthermore, due to the large amount of computer time required for the calculations, they can seldom be applied to describe the variation of the magnetic parameters in series of complexes; the density functional theories have the possibility of handling complex systems and can be used to estimate the sign and the order of magnitude of the magnetic interactions in order to substantiate all the qualitative magneto-structural correlations found in series of similar complexes.

(ii) Mixed-valence systems

A mixed valence system can generally be defined as a polynuclear transition-metal complex in which the metals appear to have more than one oxidation state [139,140]. Systems with an odd number of unpaired electrons are particularly important from a magnetic point of view. In these cases, in fact, delocalization of the unpaired electron(s) over the metal centres is associated with a stabilization of the highest multiplicity spin state [141]. The classical example of this behaviour is given by the cation $[Ni_2(napy)_4Br_2]^+$ synthesized by Sacconi and coworkers in 1974 [142]. This complex formally contains one d^9 Ni(I) and one d^8 Ni(II) which are, however, symmetry equivalent at a crystallographic level. It is commonly assumed that the "extra" electron with respect to the d^8–d^8 system is delocalized over the two metals. The ground state of the system has an $S = 3/2$ spin and the other spin state, $S = 1/2$, is thermally depopulated even at temperatures as high as 400 K [142,143].

The phenomenon of electron delocalization was already familiar to physicists from 1951 [103,144]. If we take as an example the simple three electrons (or holes) and two centre case, shown schematically in Fig. 27, we have to assume that, if the

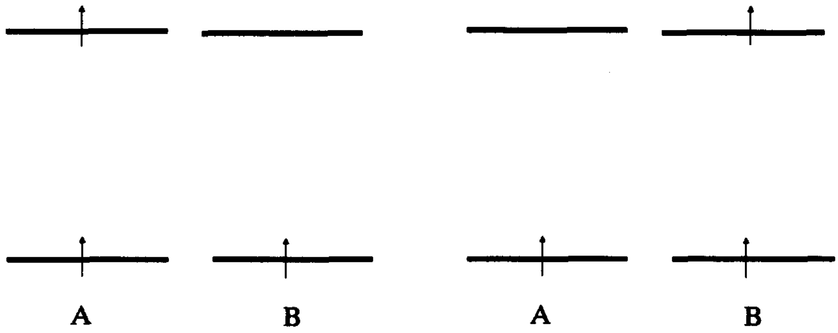

Fig. 27. Schematic representation of the spin-dependent delocalization of one electron on two metal centres.

two centres are related by a symmetry element, the two configurations with the "extra" electron localized on A or B must be equally probable. This means that we now have a double spin ladder with each total spin state, *S*, occurring twice. It is clear that the delocalization of the unpaired electron is facilitated when the electrons are all parallel. This spin-dependent electron transfer was called "double exchange" by Zener [144]. The energies of the doubled spin levels are phenomenologically accounted for in a spin hamiltonian framework with the expression

$$E_{\pm}(S)=\frac{J}{2}S(S+1)\pm B \tag{16}$$

where *B* phenomenologically accounts for the electron delocalization and is related to the energy separation between the two spin manifolds by

$$\Delta E = E_{+} - E_{-} = 2B(S+\tfrac{1}{2}) \tag{17}$$

This difference is larger for the states with the higher spin multiplicity and a large *B* can stabilize the state with the highest spin multiplicity.

We do not go further into the theory of the electronic structure of mixed valence systems here. This is indeed a matter of continuous research at the fundamental level and would require an entire review by itself. Recent advances in the phenomenological treatment of double exchange can be found in the review article by Blondin and Girerd [141], in the papers by Noodleman [145,146], and Belinskii [147,148]. Attempts to calculate the electron delocalization parameter *B* quantitatively have been performed for iron–sulphur clusters using the broken symmetry method previously described [134,135,149]. In all calculations, however, a number of approximations must be made to reduce the number of parameters to be computed.

We will conclude the review showing two systems which have been synthesized in Florence, namely the $[Fe_6(\mu_3\text{-}S)_8(PEt_3)_6]^{n+}$ complexes. These clusters are part of a series of isothermal clusters synthesized in Florence from 1981 [43–46,48], whose magnetic and electronic structure is becoming evident. The temperature dependence

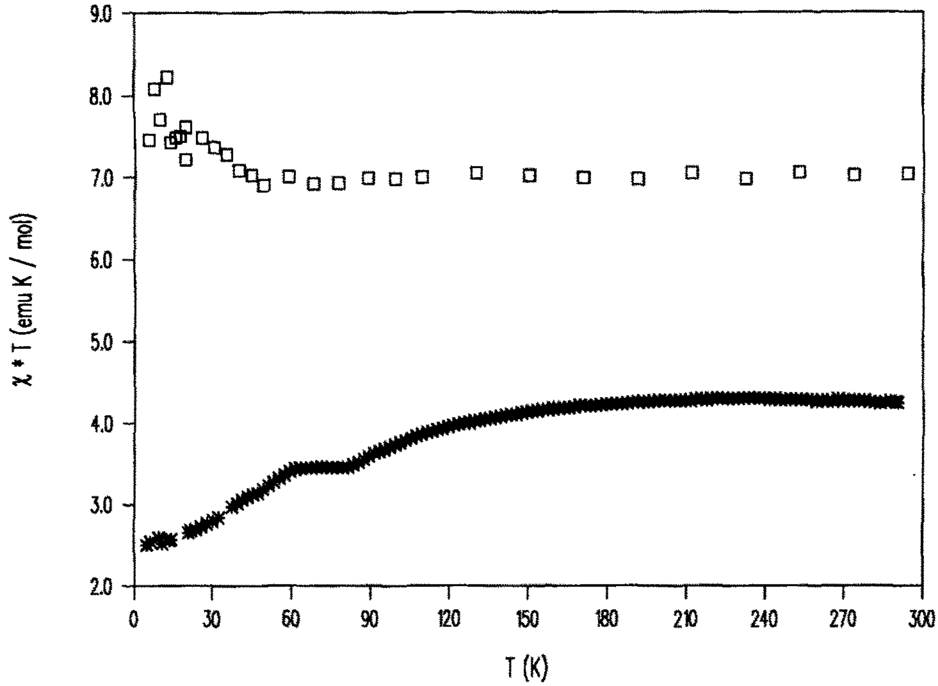

Fig. 28. Temperature dependence of the magnetic susceptibility of $[Fe_6S_8(PEt_3)_6]^+$ (upper curve) and $[Fe_6S_8(PEt_3)_6]^{2+}$ (lower curve).

of the magnetic susceptibility for $n = +1$ and $+2$ is shown in Fig. 28 [44]. The $n = +2$ clusters is formed by iron(III) centres and from Fig. 28 it is apparent that an overall antiferromagnetic interaction is operative between them, and the state of lowest multiplicity is the ground state. The $n = +1$ cluster has one electron more and the temperature dependence of χT follow a perfect Curie law except for low temperatures when intercluster interactions become operative. The observed values of the magnetic moment agree with an $S = 7/2$ spin state, showing the dramatic effect of the delocalization which forces the parallel alignment of the electrons.

ACKNOWLEDGEMENTS

The authors thank Mr. F. Cecconi, Dr. C.A. Ghilardi, and Dr. C. Zanchini for their suggestions.

REFERENCES

1 W.A. Hermann, Angew. Chem. Int. Ed. Engl., 25 (1986) 56.
2 R.H. Holm and J.A. Ibers, in W. Lovenberg (Ed.), Iron Sulfur Proteins, Vol. 3, Academic Press, New York, 1977, Chap. 7.

3 J.M. Berg and R.H. Holm, in T.G. Spiro (Ed.), Iron Sulfur Proteins, Wiley-Interscience, New York, 1982, Chap. 1.

4 P.A. Lindahl and J.A. Kovacs, J. Cluster Sci., 1 (1990) 29.

5 (a) A.F. Wells, Structural Inorganic Chemistry, Clarendon Press, Oxford, 1984.
(b) R. Chevrel, M. Hirrien and M. Sergent, Polyhedron, 5 (1986) 87.

6 (a) O. Weisser and S. Landa, Sulphide Catalysts, Their Properties and Applications, Pergamon Press, New York, 1973.
(b) B.C. Gates, J.R. Katzen and G.C.A. Schuit, Chemistry of Catalytic Processes, McGraw-Hill, New York, 1979.

7 B.A. Averill, in Metal Clusters, in L. Que, Jr. (Ed.), Proteins, ACS Symp. Ser. 372, American Chemical Society, Washington, DC, 1988, p. 258.

8 R.H. Holm, S. Ciurli and J.A. Weigel, Prog. Inorg. Chem., 38 (1990) 1.

9 D. Fenske, J. Ohmer, J. Hachgenei and K. Merzweiler, Angew. Chem. Int. Ed. Engl., 27 (1985) 1277.

10 (a) C. Floriani and G. Facchinetti, Gazz. Chim. Ital., 103 (1973) 1317.
(b) J.R. Dorfman, J.J. Girerd, E.D. Simhon, T.D.P. Stack and R.H. Holm, Inorg. Chem., 23 (1984) 4407.

11 C. Mealli, S. Midollini and L. Sacconi, Inorg. Chem., 17 (1978) 632.

12 J.J. Mayerle, S.F. Denmark, B.V. De Pamphilis, J.A. Ibers and R.H. Holm, J. Am. Chem. Soc., 97 (1975) 1032.

13 M.A. Bobrik, K.O. Hodgson and R.H. Holm, Inorg. Chem., 16 (1977) 1851.

14 A. Salifoglou, A. Simopoulos, A. Kostinas, R.W. Dunham, M.G. Kanatzidis and D. Coucouvanis, Inorg. Chem., 27 (1988) 3394.

15 C.A. Ghilardi, C. Mealli, S. Midollini, V.I. Nefedov, A. Orlandini and L. Sacconi, Inorg. Chem., 19 (1980) 2454.

16 K.S. Hagen, A.D. Watson and R.H. Holm, J. Am. Chem. Soc., 105 (1983) 3905.

17 J.-J. Girerd, G.C. Papaefthymiou, A.D. Watson, E. Gamp, K.S. Hagen, N. Edelstein, R.B. Frankel and R.H. Holm, J. Am. Chem. Soc., 106 (1984) 5941.

18 S.-B. Yu, G.C. Papaefthymiou and R.B. Holm, Inorg. Chem., 30 (1991) 3476.

19 G. Henkel, W. Tremel and B. Krebs, Angew. Chem. Int. Ed. Engl., 20 (1981) 1033.

20 K.S. Hagen, G. Christou and R.H. Holm, Inorg. Chem., 22 (1983) 309.

21 G. Henkel, M. Kriege and K. Matsumoto, J. Chem. Soc. Dalton Trans., (1988) 657.

22 A. Muller, W. Hellmann, H. Bögge, R. Jostes, M. Römer and U. Schimanski, Angew. Chem. Int. Ed. Engl., 21 (1982) 860.

23 C.A. Ghilardi, S. Midollini and L. Sacconi, Inorg. Chim. Acta, 31 (1978) L431.

24 F. Cecconi, C.A. Ghilardi and S. Midollini, Cryst. Struct. Commun., 11 (1982) 25.

25 F. Cecconi, C.A. Ghilardi, S. Midollini, A. Orlandini, A. Vacca and J.A. Ramirez, J. Chem. Soc. Dalton Trans., (1984) 773.

26 C.A. Ghilardi, S. Midollini, A. Orlandini, C. Battistoni and G. Mattogno, J. Chem. Soc. Dalton Trans., (1984) 939.

27 F. Cecconi, C.A. Ghilardi, S. Midollini and A. Orlandini, Z. Naturforsch Teil B, 46 (1991) 1161.

28 S.A. Al-Ahmad, J.W. Kampf, R.W. Dunham and D. Coucouvanis, Inorg. Chem., 30 (1991) 1164.

29 E.J. Laskowski, R.B. Frankel, W.O. Gillum, G.C. Papaefthymiou, J. Renaud, J.A. Ibers and R.H. Holm, J. Am. Chem. Soc., 100 (1978) 5322.

30 P. Barbaro, A. Bencini, I. Bertini, F. Briganti and S. Midollini, J. Am. Chem. Soc., 112 (1990) 7238.

31 M.J. Carney, G.C. Papaefthymiou, K. Spartalian, R.B. Frankel and R.H. Holm, J. Am. Chem. Soc., 110 (1988) 6084.

32 B.A. Averill, T. Herskovitz, R.H. Holm and J.A. Ibers, J. Am. Chem. Soc., 95 (1973) 3523.
33 M.A. Bobrik, E.T. Laskowski, R.W. Johnson, W.O. Gillum, J.M. Berg, K.O. Hodgson and R.H. Holm, Inorg. Chem., 17 (1978) 1403.
34 W.F. Cleland, D.A. Haltman, M. Sabat, J.A. Ibers, G.C. De Fotis and B.A. Averill, J. Am. Chem. Soc., 105 (1983) 6021.
35 G.C. Papaefthymiou, E.J. Laskowski, S. Frola-Pessôa, R.B. Frankel and R.H. Holm, Inorg. Chem., 21 (1982) 1723.
36 G.B. Wong, M.A. Bubrik and R.H. Holm, Inorg. Chem., 17 (1978) 578.
37 A. Müller, N.H. Schladerbeck and H. Bögge, J. Chem. Soc. Chem. Commun., (1987) 35.
38 M.G. Kanatzidis, D. Coucouvanis, A. Simopoulos, A. Kosticas and V. Papaefthymiou, J. Am. Chem. Soc., 107 (1985) 4925.
39 (a) T.D.P. Stack and R.H. Holm, J. Am. Chem. Soc., 110 (1988) 2484.
(b) J.A. Weigel, R.H. Holm, K.K. Surerus and E. Münck, J. Am. Chem. Soc., 111 (1989) 9246.
40 T. O'Sullivan and M.M. Miller, J. Am. Chem. Soc., 107 (1985) 4096.
41 S. Ciurli, S. Yu, R.H. Holm, K.K.P. Srivastava and E. Münck, J. Am. Chem. Soc., 112 (1990) 8169.
42 D. Fenske, J. Ohmer and J. Hachgenei, Angew. Chem. Int. Ed. Engl., 24 (1985) 993.
43 F. Cecconi, C.A. Ghilardi, S. Midollini, A. Orlandini and P. Zanello, J. Chem. Soc. Dalton Trans., (1987) 831.
44 A. Bencini and S. Midollini, unpublished results.
45 (a) F. Cecconi, C.A. Ghilardi and S. Midollini, J. Chem. Soc. Chem. Commun., (1981) 640.
(b) A. Agresti, M. Bacci, F. Cecconi, C.A. Ghilardi and S. Midollini, Inorg. Chem., 24 (1985) 689.
46 F. Cecconi, C.A. Ghilardi, S. Midollini and A. Orlandini, Inorg. Chim. Acta, 76 (1983) L183.
47 M.L. Steigerwald, T. Siegrist and S.M. Stuczynski, Inorg. Chem., 30 (1991) 2257.
48 (a) F. Cecconi, C.A. Ghilardi and S. Midollini, Inorg. Chim. Acta, 64 (1982) L47.
(b) F. Cecconi, C.A. Ghilardi, S. Midollini, A. Orlandini and P. Zanello, Polyhedron, 5 (1986) 2021.
49 D. Fenske and J. Ohmer, Angew. Chem. Int. Ed. Engl., 26 (1987) 148.
50 (a) M.G. Kanatzidis, W.R. Hagen, W.R. Dunham, R.K. Lester and D. Coucouvanis, J. Am. Chem. Soc., 107 (1985) 953.
(b) M.G. Kanatzidis, A. Salifoglou and D. Coucouvanis, Inorg. Chem., 25 (1986) 2460.
51 D. Coucouvanis, M.G. Kanatzidis, W.R. Dunham and W.R. Hagen, J. Am. Chem. Soc., 106 (1984) 7998.
52 W. Saak, G. Henkel and S Pohl, Angew. Chem. Int. Ed. Engl., 23 (1984) 150.
53 B.S. Snyder and R.H. Holm, Inorg. Chem., 29 (1990) 274.
54 M.S. Reynolds and R.H. Holm, Inorg. Chem., 27 (1988) 4494.
55 B.S. Snyder and R.H. Holm, Inorg. Chem., 27 (1988) 2339.
56 G. Christou, M. Sabat, J.A. Ibers and R.H. Holm, Inorg. Chem., 21 (1982) 3518.
57 H. Strasdeit, B. Krebs and G. Henkel, Inorg. Chem., 23 (1984) 1816.
58 H. Strasdeit, B. Krebs and G. Henkel, Z. Naturforsch Teil B, 42 (1987) 565.
59 I. Noda, B.S. Snyder and R.H. Holm, Inorg. Chem., 25 (1986) 3853.
60 D. Fenske, J. Hachgenei and J. Ohmer, Angew. Chem. Int. Ed. Engl., 24 (1985) 706.
61 S. Pohl and W. Saak, Angew. Chem. Int. Ed. Engl., 23 (1984) 907.
62 G. Christou, K.S. Hagen, J.S. Bashkin and R.H. Holm, Inorg. Chem., 24 (1985) 1010.
63 D. Fenske and J. Magull, Z. Naturforsch Teil B, 45 (1990) 121.

64 W. Saak and S. Pohl, Angew. Chem. Int. Ed. Engl., 30 (1991) 881.
65 D. Fenske, J. Ohmer and K. Mezweiler, Z. Naturforsch Teil B, 42 (1987) 803.
66 J.G. Brennan, T. Siegrist, S.M. Stuczyhski and M.L. Steigerwald, J. Am. Chem. Soc., 111 (1989) 9240.
67 (a) C.A. Ghilardi, S. Midollini and L. Sacconi, J. Chem. Soc. Chem. Commun., (1981) 47.
(b) F. Cecconi, C.A. Ghilardi and S. Midollini, Inorg. Chem., 22 (1983) 3802.
68 R.N. Mukherjee, T.D.P. Stack and R.H. Holm, J. Am. Chem. Soc., 110 (1988) 1850.
69 M.J. Carney, G.C. Papaefthymiou, R.B. Frankel and R.H. Holm, Inorg. Chem., 28 (1989) 1497.
70 M.J. Carney, G.C. Papaefthymiou, M.A. Whitener, K. Spartalian, R.B. Frankel and R.H. Holm, Inorg. Chem., 27 (1988) 346.
71 J. Gloux, P. Gloux, H. Hendriks and G. Rius, J. Am. Chem. Soc., 109 (1987) 3220.
72 J. You, B.S. Snyder, G.C. Papaefthymiou and R.H. Holm, J. Am. Chem. Soc., 112 (1990) 1067.
73 J. You and R.H. Holm, Inorg. Chem., 30 (1991) 1431.
74 J.A. Ibers and R.H. Holm, Science, 209 (1980) 223.
75 K.S. Hagen, J.G. Reynolds and R.H. Holm, J. Am. Chem. Soc., 103 (1981) 4054.
76 G. Christou and C.D. Garner, J. Chem. Soc. Dalton Trans., (1979) 1093.
77 K.S. Hagen and R.H. Holm, J. Am. Chem. Soc., 104 (1982) 5496.
78 K.S. Hagen, A.D. Watson and R.H. Holm, J. Am. Chem. Soc., 105 (1983) 3905.
79 M.G. Kanatzidis, K.S. Hagen, W.R. Dunham, R.K. Lester and D. Coucouvanis, J. Am. Chem. Soc., 107 (1985) 953.
80 S. Pohl and W. Saak, Z. Naturforsch Teil B, 43 (1988) 457.
81 G. Christou, B. Ridge and H.N. Rydan, J. Chem. Soc. Chem. Commun., (1977) 908.
82 S. Rutchik, S. Kim and M.A. Walters, Inorg. Chem., 27 (1988) 1515.
83 K.S. Hagen, A.D. Watson and R.H. Holm, Inorg. Chem., 23 (1984) 2984.
84 K. Matsumoto, N. Saiga, N. Tanaka and S. Ooi, J. Chem. Soc. Dalton Trans., (1991) 1265.
85 (a) M. Di Vaira, S. Midollini and L. Sacconi, Inorg. Chem., 16 (1977) 1518.
(b) M. Di Vaira, S. Midollini and L. Sacconi, Inorg. Chem., 18 (1979) 3466.
86 F. Cecconi, C.A. Ghilardi, S. Midollini, A. Orlandini and P. Zanello, Polyhedron, 5 (1986) 2021.
87 F. Cecconi and S. Midollini, unpublished results.
88 M. Di Vaira, S. Midollini and L. Sacconi, Inorg. Chem., 17 (1978) 816.
89 C. Bianchini, C. Mealli, A. Meli and M. Sabat, Inorg. Chem., 25 (1986) 4617.
90 F. Cecconi, C.A. Ghilardi, S. Midollini and A. Orlandini, Inorg. Chim. Acta, 84 (1991) 141.
91 D. Coucouvanis, M. Kanatzidis, E. Simhon and N.C. Baenzinger, J. Am. Chem. Soc., 104 (1982) 1874.
92 (a) P. Zanello, Coord. Chem. Rev., 83 (1988) 199.
(b) P. Zanello, Coord. Chem. Rev., 87 (1988) 1.
93 W.O. Gillum, L.E. Martenson, J.S. Chen and R.H. Holm, J. Am. Chem. Soc., 99 (1977) 584.
94 (a) L. Que, Jr., M.A. Bobrik, J.A. Ibers and R.H. Holm, J. Am. Chem. Soc., 96 (1974) 4168.
(b) G.R. Dukes and R.H. Holm, J. Am. Chem. Soc., 97 (1975) 528.
95 R.W. Johnson and R.H. Holm, J. Am. Chem. Soc., 100 (1978) 5338.
96 J.A. Weigel and R.H. Holm, J. Am. Chem. Soc., 113 (1991) 4184.
97 M. Julve, M. Verdaguer, O. Kahn, A. Gleizes and M. Philoche-Levisalles, Inorg. Chem., 22 (1983) 369.

98 K.W.H. Stevens, in R.D. Willett, D. Gatteschi and O. Kahn (Eds.), Magneto Structural Correlations in Exchange Coupled Systems, Reidel, Dordrecht, 1985, p. 105.

99 R.D. Willett, D. Gatteschi and O. Kahn (Eds.), Magneto Structural Correlations in Exchange Coupled Systems, Reidel, Dordrecht, 1985.

100 A. Bencini and D. Gatteschi, Electron Paramagnetic Resonance of Exchange Coupled Systems, Springer-Verlag, Heidelberg, 1990.

101 Y. Journaux, O. Kahn, I. Morgenstern-Badarau, J. Galy, J. Jaud, A. Bencini and D. Gatteschi, J. Am. Chem. Soc., 107 (1985) 6305.

102 L. Banci, I. Bertini, F. Briganti and C. Luchinat, New J. Chem., 15 (1991) 467.

103 P.W. Anderson, in G.T. Rado and H. Suhl (Eds.), Magnetism, Vols. 1, Academic Press, New York, 1963, p. 25.

104 (a) B. Goodenough, Phys. Rev., 100 (1955) 564.
(b) J.B. Goodenough, Phys. Chem. Solids, 6 (1958) 287.
(c) J. Kanamori, Phys. Chem. Solids, 10 (1959) 87.

105 A. Ginsberg, Inorg. Chim. Acta Rev., 5 (1971) 45.

106 P.J. Hay, J.C. Thibeault and R.J. Hoffmann, J. Am. Chem. Soc., 97 (1975) 4884.

107 O. Kahn and B. Briat, J. Chem. Soc. Faraday Trans. 2, 72 (1976) 268.

108 C. Albonico and A. Bencini, Inorg. Chem., 27 (1988) 1934.

109 (a) O. Kahn, in R.D. Willett, D. Gatteschi and O. Kahn (Eds.), Magneto-Structural Correlations in Exchange Coupled Systems, Reidel, Dordrecht, 1985, p. 37.
(b) O. Kahn, in R.D. Willet, D. Gatteschi and O. Kahn (Eds.), Magneto-Structural Correlations in Exchange Coupled Systems, Reidel, Dordrecht, 1985, p.57.

110 B.S. Snyder, G.S. Patterson, A.J. Abrahamson and R.H. Holm, J. Am. Chem. Soc., 111 (1989) 5214.

111 D. Ajò, A. Bencini and F. Mani, Inorg. Chem., 27 (1988) 2437.

112 A. Bencini, C.A. Ghilardi, S. Midollini and A. Orlandini, Inorg. Chem., 28 (1989) 1958.

113 (a) O. Kahn, Angew. Chem. Int. Ed. Engl., 24 (1985) 834.
(b) M. Verdaguer, O. Kahn, M. Julve and A. Gleizes, Nouv. J. Chim., 9 (1985) 325.
(c) R. Vicente, J. Ribas, S. Alvarez, A. Segui, X. Solans and M. Verdaguer, Inorg. Chem., 26 (1987) 4004.
(d) S. Alvarez, M. Julve and M. Verdaguer, Inorg. Chem., 29 (1990) 4500.
(e) J. Ribas, A. Garcia, R. Costa, M. Monfort, S. Alvarez, C. Zanchini, X. Solans and M.V. Domenech, Inorg. Chem., 30 (1991) 841.

114 J.R. Dorfman, J.-J. Girerd, E.D. Simhon, T.D.P. Stack and R.H. Holm, Inorg. Chem., 23 (1984) 4407.

115 P. De Loth, P. Cassoux, J.P. Daudey and J.P. Malrieu, J. Am. Chem. Soc., 103 (1981) 4007.

116 J.P. Daudey, P. De Loth and J.P. Malrieu, in R.D. Willett, D. Gatteschi and O. Kahn (Eds.), Magneto-Structural Correlations in Exchange Coupled Systems, Reidel, Dordrecht, 1985, p. 87.

117 M.F. Charlot, M. Verdaguer, Y. Journaux, P. De Loth and J.P. Daudey, Inorg. Chem., 23 (1984) 3802.

118 P. De Loth, P. Karafiloglou, J.P. Daudey and O. Kahn, J. Am. Chem. Soc., 110 (1988) 5676.

119 P. De Loth, J.P. Daudey, H. Astheimer, L. Walz and W.J. Haase, J. Chem. Phys., 82 (1985) 5048.

120 F. Nepveu, W. Haase and H. Astheimer, J. Chem. Soc. Faraday Trans. 2, 82 (1986) 551.

121 H. Astheimer and W. Haase, J. Chem. Phys., 85 (1986) 1427.

122 S. Gehring, H. Astheimer and W. Haase, J. Chem. Soc. Faraday Trans. 2, 83 (1987) 347.

123 R. Broer and W.J.A. Maaskant, Chem. Phys., 102 (1986) 103.
124 R.D. Harcourt, F.L. Skrezenek and R.G.A.R. Maclagan, J. Am. Chem. Soc., 108 (1986) 5403.
125 L. Noodleman and J.G. Norman, Jr., J. Chem. Phys., 70 (1979) 4903.
126 R.G. Parr and W. Yang, Density Functional Theories of Atoms and Molecules, Oxford University Press, Oxford, 1989.
127 L. Noodleman, J. Chem. Phys., 74 (1981) 5737.
128 K.H. Johnson, Adv. Quantum Chem., 7 (1973) 143.
129 J.C. Slater, Quantum Theory of Molecules and Solids, Vol. 4, McGraw Hill, New York, 1974.
130 A. Bencini and D. Gatteschi, J. Am. Chem. Soc., 108 (1986) 5763.
131 A. Bencini and D. Gatteschi, Chem. Phys. Lett., 156 (1989) 341.
132 A. Bencini, J. Chim. Phys., 86 (1989) 763.
133 L. Noodleman and E.J. Baerends, J. Am. Chem. Soc., 106 (1984) 2316.
134 J.G. Norman, Jr., P.B. Ryan and L. Noodleman, J. Am. Chem. Soc., 102 (1980) 4279.
135 L. Noodleman, J.G. Norman, Jr., J. Osborne, A. Aizman and D.A. Case, J. Am. Chem. Soc., 107 (1985) 3418.
136 A. Aizman and D.A. Case, J. Am. Chem. Soc., 104 (1982) 3269.
137 L. Noodleman, D.A. Case and S.F. Sontum, J. Chim. Phys., 86 (1989) 743.
138 L. Noodleman, D.A. Case and E.J. Baerends, in J.K. Labanowski and J.W. Andzelm (Eds.), Density Functional Methods in Chemistry, Springer-Verlag, Berlin, 1991, p. 109.
139 C. Creutz, Prog. Inorg. Chem., 30 (1983) 1.
140 D.B. Brown (Ed.), Mixed Valence Compounds, Reidel, Dordrecht, 1980.
141 G. Blondin and J.J. Girerd, Chem. Rev., 90 (1990) 1359.
142 L. Sacconi, C. Mealli and D. Gatteschi, Inorg. Chem., 13 (1974) 185.
143 A. Bencini, D. Gatteschi and L. Sacconi, Inorg. Chem., 17 (1978) 2670.
144 C. Zener, 82 (1951) 403.
145 L. Noodleman, Inorg. Chem., 30 (1991) 246.
146 L. Noodleman, Inorg. Chem., 30 (1991) 256.
147 M.I. Belinskii, Mol. Phys., 60 (1987) 793.
148 M.I. Belinskii and V.E. Fainzil'berg, Sov. Chem. Rev., 9 (1987) 339.
149 L. Noodleman, D.A. Case and S.F. Sontum, J. Chim. Phys., 86 (1989) 743.